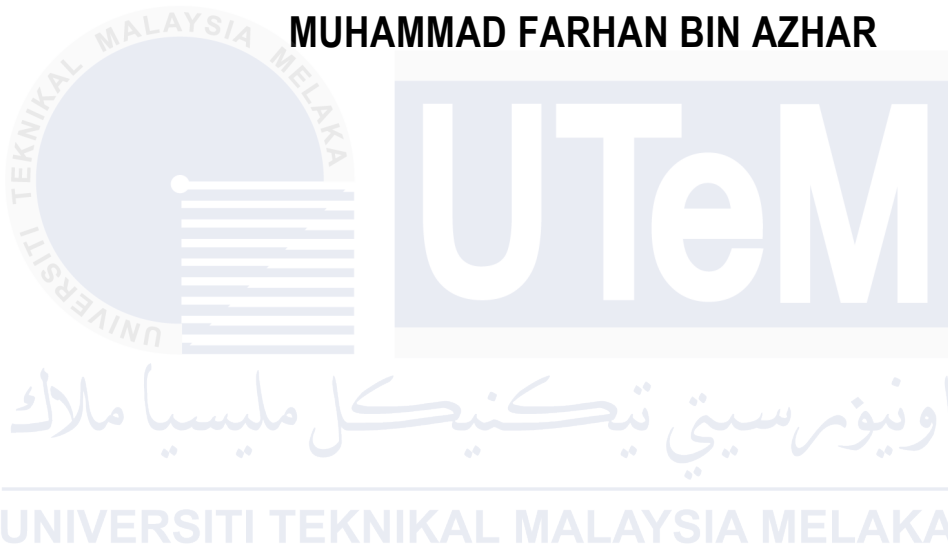


DESIGN AND ANALYSIS OF BIOMEDICAL ANTENNA USING FLEXIBLE SUBSTRATES

MUHAMMAD FARHAN BIN AZHAR



UNIVERSITI TEKNIKAL MALAYSIA MELAKA

DESIGN AND ANALYSIS OF BIOMEDICAL ANTENNA USING FLEXIBLE SUBSTRATES

MUHAMMAD FARHAN BIN AZHAR

**This report is submitted in partial fulfilment of the requirements for
the degree of Bachelor of Electronics Engineering Technology with
Honours**

**Faculty of Electronics and Computer Technology and Engineering
Universiti Teknikal Malaysia Melaka**

UNIVERSITI TEKNIKAL MALAYSIA MELAKA

2025

BORANG PENGESAHAN STATUS LAPORAN
PROJEK SARJANA MUDA II

Tajuk Projek : DESIGN AND ANALYSIS OF BIOMEDICAL
ANTENNA USING FLEXIBLE SUBSTRATES
Sesi Pengajian : 2023/2024

Saya MUHAMMAD FARHAN BIN AZHAR mengaku membenarkan laporan Projek Sarjana Muda ini disimpan di Perpustakaan dengan syarat-syarat kegunaan seperti berikut:

1. Laporan adalah hakmilik Universiti Teknikal Malaysia Melaka.
2. Perpustakaan dibenarkan membuat salinan untuk tujuan pengajian sahaja.
3. Perpustakaan dibenarkan membuat salinan laporan ini sebagai bahan pertukaran antara institusi pengajian tinggi.
4. Sila tandakan (✓):

☐

SULIT*

(Mengandungi maklumat yang berdarjah keselamatan atau kepentingan Malaysia seperti yang termaktub di dalam AKTA RAHSIA RASMI 1972)

☐

TERHAD*

(Mengandungi maklumat terhad yang telah ditentukan oleh organisasi/badan di mana penyelidikan dijalankan).

☐

TIDAK TERHAD

Disahkan oleh:

(TANDATANGAN PENULIS)

Alamat Tetap: _____

Tarikh : 21 Januari 2025

Tarikh : 21 Januari 2025

*CATATAN: Jika laporan ini SULIT atau TERHAD, sila lampirkan surat daripada pihak berkuasa/organisasi berkenaan dengan menyatakan sekali tempoh laporan ini perlu dikelaskan sebagai SULIT atau TERHAD.



DECLARATION

I declare that this project report entitled “DESIGN AND ANALYSIS OF BIOMEDICAL ANTENNA USING FLEXIBLE SUBSTRATES” is the result of my own research except as cited in the references. The project report has not been accepted for any degree and is not concurrently submitted in candidature of any other degree.

Signature :

Student Name :

MUHAMMAD FARHAN BIN AZHAR

Date :

21/1/2025

UNIVERSITI TEKNIKAL MALAYSIA MELAKA

APPROVAL

I hereby declare that I have checked this project report and in my opinion, this project report is adequate in terms of scope and quality for the award of the degree of Bachelor of Electronics Engineering Technology with Honours.

Signature :

Supervisor Name :

DR. HASLINAH BINTI MOHD

Date :

21/12025

Signature :

Co-Supervisor :

Name (if any)

Date :

DEDICATION

*To my beloved mother, Latita Binti Ahamd, and father, Azhar Bin Mohd Zain,
and
my other family member.*



ABSTRACT

Flexible substrates, such as polymers, textiles, and elastomers, are widely utilized in wearable applications due to their ability to conform to the human body and endure mechanical deformations, including bending, stretching, and twisting. However, their inherent characteristics, such as higher dielectric losses and lower mechanical stability, present significant challenges in antenna design, often leading to degraded performance. This project investigates advanced antenna design techniques to develop high-performance antennas optimized for biomedical applications. The study includes the determination of key antenna parameters for operation at the desired resonance frequency which is 4.5 GHz, with a focus on impedance matching, radiation pattern, and efficiency. The initial stages involved an extensive review of flexible substrates and MIMO antenna technologies from academic and industrial sources. Subsequently, antennas were designed and analyzed using CST Studio Suite, with and without the integration of Defected Ground Structure (DGS). The performance of the antennas for wearable biomedical applications was assessed through simulations. Using CST Studio Suite, antennas with and without DGS were developed and analyzed. Simulation findings revealed that the antenna with DGS included had a return loss of -19.84 dB, a substantial improvement over the antenna without DGS, which had a return loss of -8.19 dB. Even with more antenna elements in a linear array, the MIMO antenna showed a consistent bandwidth of 0.0632 GHz. Critical factors like size, shape, and material qualities were successfully optimized in this study, demonstrating that antennas may provide high accuracy and consistent performance metrics that are validated for integration with medical devices. A key factor in reaching these outcomes was the simulation-based design with CST Studio Suite, which removed the need for initial manufacturing and paved the road for high-performance biomedical antenna systems. Future research will investigate different flexible substrates, such as polyimide or LCP, to improve biocompatibility and durability that incorporate sophisticated sensing capabilities for data transfer and health monitoring which create miniature antennas using contemporary fabrication methods to guarantee smooth integration into daily life. This project lays the groundwork for creative and effective antenna systems, advancing healthcare delivery and medical technologies.

ABSTRAK

Substrat fleksibel seperti polimer, tekstil, dan elastomer sering digunakan dalam aplikasi kerana keupayaannya untuk menyesuaikan diri dengan bentuk tubuh manusia dan menahan perubahan mekanikal seperti lenturan, regangan, dan putaran. Walau bagaimanapun, ciri-ciri semula jadinya, seperti kehilangan dielektrik yang lebih tinggi dan kestabilan mekanikal yang lebih rendah, menimbulkan cabaran besar dalam reka bentuk antenna, yang sering menyebabkan penurunan prestasi. Projek ini mengkaji teknik reka bentuk antenna yang maju untuk membangunkan antenna berprestasi tinggi yang dioptimumkan untuk aplikasi bioperubatan. Kajian ini merangkumi penentuan parameter utama antenna untuk operasi pada frekuensi resonans yang dikehendaki iaitu 4.5 GHz, dengan penekanan pada padanan impedans, corak pancaran, dan kecekapan. Peringkat awal melibatkan kajian menyeluruh tentang substrat fleksibel dan teknologi antenna MIMO daripada sumber akademik dan industri. Seterusnya, antenna direka dan dianalisis menggunakan perisian CST Studio Suite, dengan dan tanpa integrasi Struktur Tapak Cacat (Defected Ground Structure, DGS). Prestasi antenna untuk aplikasi bioperubatan boleh pakai dinilai melalui simulasi. Hasil simulasi menunjukkan antenna dengan DGS mempunyai kerugian pantulan sebanyak -19.84 dB, peningkatan ketara berbanding antenna tanpa DGS yang mencatatkan kerugian pantulan sebanyak -8.19 dB. Walaupun dengan elemen antenna yang lebih banyak dalam susunan linear, antenna MIMO menunjukkan jalur lebar yang konsisten sebanyak 0.0632 GHz. Faktor-faktor kritikal seperti saiz, bentuk, dan sifat bahan berjaya dioptimumkan dalam kajian ini, menunjukkan bahawa antenna mampu memberikan ketepatan tinggi dan metrik prestasi yang konsisten, yang disahkan untuk integrasi dengan peranti perubatan. Faktor utama kejayaan ini adalah reka bentuk berasaskan simulasi, yang menghapuskan keperluan pembuatan awal dan membuka jalan untuk sistem antenna bioperubatan berprestasi tinggi. Penyelidikan masa hadapan akan mengkaji pelbagai substrat fleksibel seperti polimida atau LCP untuk meningkatkan biokeserasian dan ketahanan, termasuk keupayaan penderiaan canggih untuk pemindahan data dan pemantauan kesihatan, serta menghasilkan antenna bersaiz kecil menggunakan kaedah fabrikasi moden bagi memastikan integrasi yang lancar dalam kehidupan seharian. Projek ini meletakkan asas untuk sistem antenna yang inovatif dan berkesan, sekaligus memajukan penyampaian penjagaan kesihatan dan teknologi perubatan.

ACKNOWLEDGEMENTS

First and foremost, I would like to express my gratitude to my supervisor, DR. HASLINAH BINTI MOHD NASIR for her precious guidance, words of wisdom and patience throughout this project.

I am also indebted to Universiti Teknikal Malaysia Melaka (UTeM) for the financial support to accomplish the project. Not forgetting my fellow colleague, AHMAD FAKHRULLAH BIN ABDUL RAZAK for the willingness to share his thoughts and ideas regarding the project.

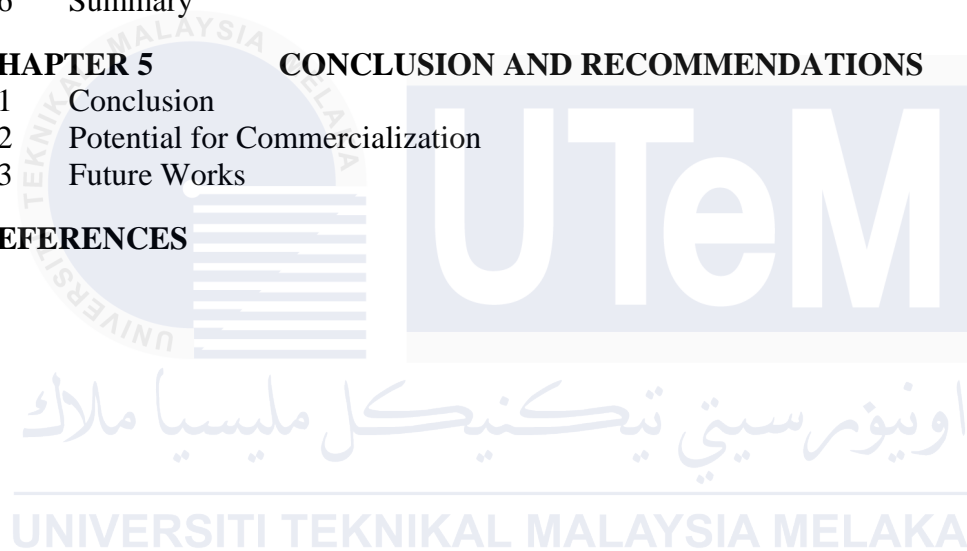
My highest appreciation goes to my parents and family members for their love and prayers during the period of my study. And to DR. MUHAMMAD INAM ABBASI, thanks for the help and guidance regarding the technical knowledge needed for the completion of this project.

Finally, I would like to thank all the staff at the Faculty of Electronics & Computer Technology & Engineering, colleagues and classmates, the faculty members, as well as other individuals who are not listed here for being co-operative and helpful.

TABLE OF CONTENTS

	PAGE
DECLARATION	
APPROVAL	
DEDICATIONS	
ABSTRACT	i
ABSTRAK	ii
ACKNOWLEDGEMENTS	iii
TABLE OF CONTENTS	iv
LIST OF TABLES	vi
LIST OF FIGURES	vii
CHAPTER 1 INTRODUCTION	10
1.1 Background	10
1.2 Enhancing Global Healthcare Accessibility with Flexible Substrate Biomedical Antennas for Advanced Medical Monitoring	11
1.3 Problem Statement	11
1.4 Project Objective	12
1.5 Scope of Project	12
CHAPTER 2 LITERATURE REVIEW	13
2.1 Introduction	13
2.2 MIMO Antenna	14
2.2.1 Types of Biomedical Antennas used in the medical field	15
2.2.2 Wearable Antenna	15
2.3 Flexible Substrates	16
2.3.1 PET Material	19
2.4 Analyzing several techniques for designing advanced antennas to improve performance and flexibility.	22
2.5 Summary	39
CHAPTER 3 METHODOLOGY	40
3.1 Introduction	40
3.2 Selecting and Evaluating Tools for Sustainable Development	40
3.3 Project flow chart	41
3.4 Experimental Setup	44
3.5 Antenna Design	45
3.5.1 Evaluation of flexible substrates	46
3.5.2 Design and Analysis of high-performance Antenna	46
3.5.3 Run the simulation and analyze the antenna output	46

3.5.4	Theoretical Dimension	47
3.5.5	Dimensions of the designed antenna after optimization	52
3.6	Designing MIMO antenna	54
3.7	Limitation of purposed Methodology	55
3.8	Summary	56
CHAPTER 4	RESULTS AND DISCUSSIONS	58
4.1	Introduction	58
4.2	Result and analysis by using Theoretical value	59
4.3	Result and analysis of antenna without DGS	60
4.4	Result and analysis of antenna with DGS	64
4.5	Result and Analysis of MIMO Antenna (Linear Array)	69
4.6	Summary	71
CHAPTER 5	CONCLUSION AND RECOMMENDATIONS	73
5.1	Conclusion	73
5.2	Potential for Commercialization	74
5.3	Future Works	75
REFERENCES		77



LIST OF TABLES

TABLE	TITLE	PAGE
Table 2.1:	Summary of optical transparent antennas using thin film [9]	17
Table 2.2:	Summary of optical transparent antennas using mesh grid [9]	18
Table 2.3:	Review of the previous Studies about Flexible antenna with different applications [11]	20
Table 2.4:	Parametric analysis of the MIMO antenna [3]	22
Table 2.5:	Formula used by Abbasi et al. [3]	26
Table 2.6:	Comparison with previous recent works [3]	28
Table 2.7:	Peak Antenna Gain of an Inkjet-Printed Antenna [12]	32
Table 2.8:	Comparison table improvement of the antenna with and without DGS [13]	33
Table 2.9:	Comparison table of the antenna to benchmark with existing work [13]	34
Table 2.10:	Physical dimensions of the proposed antenna [13]	37
Table 2.11:	Comparison table of the research paper	38
Table 3.1:	Parameter of microstrip patch antenna	53
Table 4.1:	Comparison table of the antenna at the antenna without and with DGS	68

LIST OF FIGURES

FIGURE	TITLE	PAGE
Figure 2.1:	PET film with a flexible inkjet-printed antenna [12]	21
Figure 2.2:	Parametric analysis for metal mesh lattice size of the proposed transparent and flexible MIMO antenna (a) $l = 1\text{mm}$, $w = 0.1$ to 0.3mm , (b) $l = 2\text{mm}$, $w = 0.1$ to 0.3mm , (c) $l = 3\text{mm}$, $w = 0.1$ to 0.3mm [3]	22
Figure 2.3:	(a) Fabricated prototype of the proposed transparent MIMO antenna, (b) measured scattering parameters for the proposed transparent and flexible MIMO antenna [3]	25
Figure 2.4:	Radiation pattern of the transparent MIMO antenna at 4.5 GHz (a) E-plane, (b) H-plane [3]	27
Figure 2.5:	The ECC and DG performance of the transparent and flexible MIMO antenna (a) simulated, (b) measured [3]	28
Figure 2.6:	The S_{11} plot of the PET film flexible inkjet-printed antenna [12]	29
Figure 2.7:	Simulated and measured normalized radiation patterns of the flexible inkjet printer antenna at distinct frequencies of the operating range antenna [12]	31
Figure 2.8:	S-parameter of the antenna with and without DGS at the resonant frequency [13]	33
Figure 2.9:	VSWR of the proposed antenna [13]	33
Figure 2.10:	S-parameter of the linear array, (a) 1×2 array, (b) 1×4 array, (c) 1×8 array [13]	35
Figure 2.11:	Formula used to calculate parameter [13]	36
Figure 2.12:	Researcher Proposed antenna geometry, (a) top view, (b) ground view [13]	37
Figure 2.13:	The linear antenna array, (a) front view of the 1×2 array, (b) back view of 1×2 array, (c) front view of the 1×4 array, (d) back view of 1×4 array, (e) front view of the 1×8 array, (f) back view of 1×8 array [13]	37
Figure 3.1:	Flow chart of Project	43

Figure 3.2: (a)Front view of the proposed antenna, (b)Back view, and (c)Perspective view	45
Figure 3.3: (a) Front view (b) Normal Ground (c) DGS Ground (Slot DGS)	51
Figure 3.4: Detail parameter of microstrip antenna after the optimization process (a)Front view (b)Back view	52
Figure 3.5: (a)1 x 2 array antenna (b)1 x 3 array antenna (c)1 x 4 array antenna	54
Figure 4.1: Result of S-Parameter from proposed design microstrip antenna (Calculated Parameter)	59
Figure 4.2: Result obtained during parameter sweep	60
Figure 4.3: S-Parameter analysis to obtain Return Loss	61
Figure 4.4: S-Parameter analysis to obtain Bandwidth	61
Figure 4.5: VSWR	62
Figure 4.6: Surface current antenna at resonant frequency	62
Figure 4.7: (a)Radiation pattern in 3-D form (b)Radiation pattern in Polar form	63
Figure 4.8: Max Gain over frequency for the whole Bandwidth	64
Figure 4.9: S-Parameter analysis to obtain Return Loss	65
Figure 4.10: S-Parameter analysis to obtain Bandwidth	65
Figure 4.11: VSWR	66
Figure 4.12: Surface current antenna at resonant frequency	66
Figure 4.13: (a)Radiation pattern in 3-D form (b)Radiation pattern in Polar form	67
Figure 4.14: Max Gain over frequency for the whole Bandwidth	68
Figure 4.15: (a)Front view (b) Back view of 1 x 2 array antenna	69
Figure 4.16: S-Parameter of 1 x 2 array antenna	70
Figure 4.17: (a)Front view (b) Back view of 1 x 3 array antenna	70
Figure 4.18: S-Parameter of 1 x 3 array antenna	70
Figure 4.19: (a)Front view (b) Back view of 1 x 4 array antenna	71
Figure 4.20: S-Parameter of 1 x 4 array antenna	71

CHAPTER 1

INTRODUCTION

1.1 Background

Wearable electronics are bringing about an eruption in the way we perceive technology. Using a synergy of bendable electronics and flexible textiles, researchers are building wearable devices that can detect, communicate, and even collect energy [1]. This increase of interest in wearable sensors with antennae stems from the fact that they are easy to manufacture, can be applied for different sensing tasks, and are cheaper than other devices. Even though developing an antenna with good performance is the result of carefully considering factors such as operating environment, frequency band, and power transmission, it is not easy. Material selection is also important as the textile substrate should be highly flexible, and the conductive elements should have the least resistance and be durable enough to wear and tear [2]. Wearable antennas also have huge potential in healthcare by tracking human motion and physiological changes and helping in disease detection and remote patient monitoring. Multiple-input multiple-output (MIMO) antennas have emerged as a promising solution in this domain due to their ability to improve data transmission rates, enhance channel capacity, and ensure reliable communication in multipath environments. These advantages make MIMO systems highly suitable for wearable biomedical applications, where real-time monitoring and data transmission are critical. This project focuses on the development of a MIMO antenna using a flexible substrate specifically for variable biomedical applications. It can serve as a fundamental basis for future studies and advancements in this field.

1.2 Enhancing Global Healthcare Accessibility with Flexible Substrate Biomedical Antennas for Advanced Medical Monitoring

The design and analysis of the proposed biomedical antennas on flexible substrates aim to improve the technology so that it can be smartly implantable within the human body. Antennas are mounted over flexible substrates, which enables them to be flexed and adapted over curved and complex body shapes, thus forming a practically transparent part of wearable medical devices. The net effect is to not only ensure that the user is comfortable but that the antennas can perform well by enhancing the ability of the antenna to avoid system performance degradation associated with signal loss through the use of multiple-input and multiple-output (MIMO) arrays and adaptive beamforming. Subsequently, it can enhance the reliability and accessibility of medical telemetry and monitoring systems. Ultimately, we hope to improve medical technology by enhancing the comfort, reliability, and efficacy of the healthcare devices by which patients are administered medical treatment via the developed design and analysis of biomedical antennas on flexible substrates.

1.3 Problem Statement

Wearable antennas require materials that are lightweight, flexible, and biocompatible to ensure user comfort and device performance. Flexible substrates, such as polymers, textiles, and elastomers, are commonly used due to their ability to conform to the human body and withstand mechanical deformations like bending, stretching, and twisting. However, the use of flexible substrates introduces several challenges in antenna design. These materials often exhibit higher dielectric losses and lower mechanical stability, which can degrade the antenna's performance [2]. Addressing these issues requires innovative design approaches that consider the mechanical and electromagnetic properties of flexible substrates. This research aims to design and analyze antennas using flexible substrates for

wearable biomedical applications, focusing on optimizing performance under dynamic conditions, enhancing durability, and minimizing the impact of body interactions. By overcoming these challenges, this study seeks to advance the development of reliable and efficient antennas for next-generation wearable devices.

1.4 Project Objective

The project aims to advance the field of antennas while applying it in the medical field making healthcare devices more comfortable, reliable, and effective, ultimately contributing to improved healthcare delivery and patient outcomes globally. The objectives are as follows:

- a) To study advanced antenna design techniques aimed at producing high-performance antennas.
- b) To design an antenna by determining its parameters to operate at the planned resonance frequency.
- c) To analyze a specifically designed for biomedical applications, focusing on impedance matching, radiation pattern, and efficiency.

1.5 Scope of Project

The scope of this project are as follows:

- a) Research and evaluate flexible substrates and MIMO antennas from diverse academic and industry sources.
- b) Design and analyze high-performance antennas using CST Studio Suite.
- c) Conduct simulations and thoroughly analyze the antenna performance results for wearable biomedical applications.

CHAPTER 2

LITERATURE REVIEW

2.1 Introduction

The proposed project pioneered the use of flexible substrates for the development of next-generation biomedical antennas. This paper seeks to give a brief explanation of the study, the reason for the study, the objectives of the study, the research questions used in the study, the methodology used in the study, the findings of the study, and the contribution of the study towards the existing knowledge. It reviews the literature, examines the problem and gaps in the existing literature, and describes how the research proposed in this proposal would advance the body of knowledge about the factors that have to be taken into consideration to design a proper MIMO antenna. In particular, this work is devoted to the design and modelling of biomedical antennas based on flexible substrates. This research provides recommendations on improving the effectiveness of antennas through the measurement of the antenna output and the antenna tuning done using CST Studio Suite. Additionally, the study shows how this information builds on prior sources of research in the field. Before designing a MIMO microstrip patch antenna, it is imperative to identify the operating frequency and choose the right material for the MIMO antenna, and then take into account other crucial parameters like VSWR, balance, efficiency, far-field patterns, and S-parameters. This is more so given the fact that flexible substrates could be of immense value when used in biomedical applications since they can easily be made to conform to the shape of the body and are generally more comfortable for the patient.

2.2 MIMO Antenna

MIMO (Multiple-Input Multiple-Output) is a complex antenna technique employed in modern wireless communication systems to increase data rates and link distance without using any extra spectrum or transmit power. MIMO systems employ many antennas on both the transmitter and receiver side to exploit multipath propagation, in which the transmitted signal is reflected off objects and received at the receiver through multiple paths. This creates a multipath environment, which is generally considered undesirable in wireless communication but is used to the advantage of MIMO. Based on research by Abassi et al., the utilization of a wired metal mesh with a square lattice on a 0.1 mm thick transparent and flexible PET material substrate for patch elements in close proximity. The proposed MIMO antenna design demonstrates comparable performance with significantly closed spacing between antenna elements compared to previous works [3].

Similarly, Qiu et al. explore the development of compact, transparent, and flexible antennas for wearable devices in 5G networks. Their research utilizes Ni-based embedded metallic mesh (EMM) nanotechnology along with simulation and measurement techniques for evaluating antenna performance. The observation from their research shows superior transparency (93%) and radiation efficiency (up to 85%) of the designed 5G MIMO antenna and Isolation above 20 dB, envelope correlation coefficient under 0.005, operation in 5G band [4].

Utilized a micro-metal mesh conductive film for the antenna design. MIMO antenna designs are also being explored using flexible materials. Li et al. propose a MIMO antenna design using micro-metal mesh conductive film for dual-band WLAN applications, utilizing a specific substrate and microstrip lines in the fabrication process. Their proposed antenna demonstrated high efficiency and peak gain at dual bands [5].

2.2.1 Types of Biomedical Antennas used in the medical field

Biomedical antennas can be broadly categorized into three primary types based on their integration with the human body that is ingestible, wearable, and implantable. Each category offers unique advantages and considerations for specific biomedical applications. For example, Sulaiman et al. present a low-profile and compact implantable antenna designed for medical applications with minimal radiation absorption by the body. Their research employs a meander line technique with an open loop configuration and simple transmission line feeding. They achieved a significant size reduction (79% compared to previous work) while maintaining satisfactory performance with a 10 dB bandwidth of 6.17% and a maximum gain of -22 dBi. The antenna also demonstrated compliance with IEEE safety guidelines, with a maximum of 1g and averaged 10g Specific Absorption Rate (SAR) of 74.7 W/kg and 17.7 W/kg, respectively, and an Equivalent Isotropic Radiated Power (EIRP) of -25.28 dBi [6].

2.2.2 Wearable Antenna

This project is centred on body wearable antennas attached externally to the human body, like on apparel or ornaments. This makes it possible to have a steady flow of data transfer or health status check-ups without affecting the wearer's comfort. Developing wearable antennas due to their potential to revolutionize the functionality and capabilities of wearable devices. These antennas, designed to be transparent and flexible, can be seamlessly integrated into clothing and accessories. This paves the way for creating next-generation wearables that are compact, comfortable, and aesthetically pleasing. Furthermore, wearable antennas can significantly boost signal strength and data speeds, especially for devices utilizing 5G. This enhanced wireless communication is essential for applications demanding reliable and fast data transmission, such as healthcare

monitoring and the Internet of Things (IoT) [3].

Valuable insights into the current state-of-the-art can be found in review papers by Ali et al. which analyze critical design issues and challenges, suitable materials for wearable antennas, human body interaction with antennas, and SAR analysis, providing a comprehensive review of design considerations, materials, and safety aspects of wearable antennas [7].

2.3 Flexible Substrates

Flexible substrates are thin and heat-resistant polymers and comprise polyimide, Kapton polyimide substrate, and Polyethylene Terephthalate (PET). They are incorporated in printed circuit boards (PCBs) to enable the passing of signals between the user interface and the storage system. Flexible substrates are particularly important in modern computing and electronic equipment because they are bendable and can, therefore, be fitted in small and tight spaces. All in all, flexible substrates offer substantial benefits over conventional PCBs, including lower weight, easy installation, and higher reliability.

Research Khan et al. extends beyond just transparent and flexible designs and proposes a 4x4 microstrip antenna array on flexible Kapton polyimide substrate for 16 GHz WPT, investigating the design and simulation of antenna arrays on flexible substrates for wireless power transfer applications. The research focuses on achieving a broadside gain of 16.38 dB, a 10 dB bandwidth of 240 MHz, a beam width of 29.48 degrees, and a scanning range of ± 158 degrees [8].

Chisti et al. delve deeper, analyzing different antenna designs and technologies, and providing a comparison of optically transparent antennas, performance metrics, and technological advancements. The choice of substrate material helps achieve transparency, though it compromises the antenna's conductivity as observed in Table 2.1 and Table 2.2.

The dimensions of the patch influence the resonance frequency, radiation characteristics, and physical size, as well as their relationship to wavelengths and conduction losses [9].

Table 2.1: Summary of optical transparent antennas using thin film [9]

Ref.	Freq (GHz)	Substrate Material	Sub Thickness	Patch Material	Gain (dBi)	Bandwidth	Efficiency (%)	Transparency	Transmittance
[5]	5–18	PDMS	-	Fabric tissue (F)	3.2–4.2	0.1–25 GHz	66–90	-	-
[6]	23–30	Polyester fabric (F)	0.35 mm	Copper foil	4.2	24–28 GHz	-	-	-
[7]	10	Alumina	100 μ m	Polyaniline /copper	1.8, 4.69	9.6–9.9 GHz	56, 98	-	-
[8]	0.9	PET (F)	0.5 mm	Copper /CP (F)	3	0.8–0.95 GHz	-	-	-
[9]	2.4	Glass	-	AZO/AgNWs	-	2–3.5 GHz	-	-	80.28
[10]	45	Quartz	5 mm	AZO (F)	-	43–46.5 GHz	-	86	83
[11]	2.4	Silicon	-	AZO	4.9	-	-7.3 dBi	-	-
[12]	2.53	Glass	2 mm	AgHT-4	9.8	2.49–2.58 GHz	-	-	75
[13]	28	Glass	2.54 mm	ITO, FTO, AgHT-4, AgHT-8	4.8, 4.2, 4.4, 4.2	26–36 GHz	81, 73, 75, 73	-	-
[14]	3.5	Glass	2.3 mm	AgHT-4	3.96	3.49–3.55 GHz	50	-	92
[15]	5.25	Polyimide	-	IZTO/Ag /IZTO	4.1–5.2	4.7–5.7 GHz	61–82	-	-
[16]	9.85	Quartz glass	1.5 mm	ITO	4.27	-	56	-	-
[17]	5.8	Glass	1 mm	ITO	6	5.7–6 GHz	-	-	-
[18]	0.1–1 THz	Polyimide	0.013 mm	Polymer	-	-	-	-	80
[19]	3, 5, 8, 13	Borosilicate glass	7 nm	Cu, ITO	-4, -2, 0.5, 2	3.1–10.6 GHz	27, 25, 20, 18	88	-
[20]	24.8	Pyrex glass	0.4 μ m	ITO	11.5	17–30 GHz	92.30	-	-
[21]	2.45	Soda-lime glass	2 mm	MM	-	2–3 GHz	-	-	75
[22]	2	Corning glass	1.1 mm	AgGL	5.2	19.7%	60	51–70	-
[23]	1–8.5	Perspex	2 mm	AgHT-4	-2.5 to -33	1–10 GHz	-	-	-
[24]	2, 6	Corning glass	1.1 mm	AgGL	2–6	2.5–5.3 GHz	-	80	-
[25]	750	Polyimide	20 μ m	ITO,TIO with MWCNT	4.5–5.8	723–780 GHz	47–61	-	-
[26]	23.92–43.8	Plexiglass	1.48 mm	-	2.8	23.92–43.8 GHz	90	-	-
[27]	2.4	Silica glass	1.4 μ m	GZO	-	-	-	-	-
[28]	2.5, 5	Pyrex glass	4 mm	FTO	0.43, 3.63	-	72	-	74–84
[29]	2.45, 5.8	PET	0.175 mm	AgHT-8	-3.25, -4.53	1.6–2.95, 5.4–6.4	-	80	-
[30]	4.9	Soda-lime glass	-	FTO	5.16	0.8 GHz	-	-	60
[31]	2.4	PET	0.05 mm	ITO	-1.36	2.2–3 GHz	20–52	96	-

Table 2.2: Summary of optical transparent antennas using mesh grid [9]

Ref	Freq (GHz)	Substrate Material	Sub Thickness	Patch Material (Mesh)	Gain (dBi)	Bandwidth	Efficiency (%)	Transparency	Transmittance
[32]	0.84	Glass	0.006 mm	Ag/Ti	-	-	85	81	-
[33]	2.4–2.5	Acrylic	1.2 mm	Metal mesh	4.14	2.48–2.52 GHz	56	82	-
[34]	18	Quartz	-	ITO/metal mesh	-	-	38, 41	-	73–95, 66–94
Ref	Freq (GHz)	Substrate Material	Sub Thickness	Patch Material (Mesh)	Gain (dBi)	Bandwidth	Efficiency (%)	Transparency	Transmittance
[35]	2.46–2.94	Fused silica	-	Tortuous MM	−3.4	2.82–3.0 GHz	81	-	30–45
[36]	3.45	PDMS	2–4 mm	EGaIn (liquid metal)	-	3.3–3.5 GHz	60	-	-
[37]	2.4–2.48, 5.15–5.8	Glass	1.09 mm	MMMC	0.74, 2.30	-	43, 46	-	75
[38]	2.43–2.48	Borosilicate glass	4, 3.5, 3, 2.5 mm	Meshed patch	4.4	2.39–2.58 GHz	-	74	-
[39]	2.3–3	PET/PMMA	4–5 mm	Metal mesh	6	2.4–2.9 GHz	90	70	-
[40]	2.33–2.53, 4.7–5.6	PDMS	3 mm	Mesh	2.2, 3.1	170–200 MHz, 700–900 MHz	37, 44	-	50–70
[41]	2.4–2.5	Acrylic	1 mm	Micromesh	4.75, −4.23, and 2.63	2.4–2.6 GHz	66.32, 7.76, and 42.69	80	-
[42]	60	Thick fused silica 7980 Corning	0.2 mm	Al-MM	3.20	53.55 GHz	-	78	-
[43]	2.4, 2.55	Quartz	2.25 mm	Silver epoxy mesh	4.94, 7.23	2.4–2.6 GHz	-	90	-
[44]	28	Glass	0.7 mm	Ag-alloy (diamond-shaped)	9.16	27.5–29.5 GHz	52	41	-
[45]	2–2.5	Plexiglass	2.03 mm	Meshed copper	7.32	-	78	70–95	-
[46]	27–35	Acrylic	2 mm	Cu micro-grids	-	27–35 GHz	-	-	-
[47]	0.5–20	PET	0.1 mm	Metal mesh	10.4	0.78–20 GHz	-	-	72
[48]	22–40	COPs	0.1 mm	Thin MM	1.12	24–29 GHz, 35.5–37.5 GHz	34–43	92–98	-
[49]	6.63, 7.291, 7.29, 7.22	FR-4	1.62 mm	MWCNT	8.8	4.5–8.5 GHz	86	-	-

Prades et al. explore diverse flexible substrate materials like silver nanoparticle ink, ceramic-polymer composites, conductive polymers, metamaterial-based structures, and copper-plated nylon fabric. The technologies covered different frequency bands, including NFC, UHF RFID, satellite systems, DVB-H, GSM, UMTS, WLANs, Bluetooth, Ultra-

Wideband (UWB), and scientific applications at the Ku-band. Their research addressed the use of diverse materials and technologies in various frequency bands, reflecting the active research momentum in flexible substrate antennas [10].

2.3.1 PET Material

PET is a type of plastic that is used in packaging and garment industries, among others. It is a thermoplastic polyester that is synthesized by the esterification of ethylene glycol and terephthalic acid. PET is among the most used materials due to its strength, durability, and chemical and heat-resistant nature. It has continued to be used in biomedical applications, such as the use of flexible antennas in the manufacturing of medical devices. These antennas, which are usually incorporated in wearable health monitoring devices, implants, and diagnostic tools, are enhanced by PET's biocompatibility and mechanical properties. Heat resistance and stability of PET are necessary to ensure that it performs uniformly in various physiological environments with varying temperatures and chemical susceptibilities. In Table 2.3 it shows the previous studies about Flexible antennae with different applications. Al-Haddad et al. review fabrication techniques such as screen printing, inkjet printing, sewing, and embroidering techniques for flexible antennas highlighting the importance of conductive materials like silver and substrates like PET [11].

Table 2.3: Review of the previous Studies about Flexible antenna with different applications [11]

Ref.	Type of the antenna	Substrate	Fabrication method	Application	Advantages
[8]	Monopole antenna	polyethylene terephthalate (PET)	Inkjet printer DMP-3000	Wearable devices at 1.8 GHz	Obtained efficiency of 93.33%. The proposed design can overcome the cost and size.
[50]	RFID	Thermoplastic polyurethane (TPU)	Screen printing	Radio frequency	The antenna shows a good performance with high elongation. Simulation and experiment results were excellently matched.
[63]	Microstrip patch	Polydimethylsiloxane (PDMS)	Embroidery	Realization of Robust Passive and Active Flexible Wearable Antennas at ISM 2.45GHz	Consistence performance. The antenna could be reconfigurable Experienced no performance change after exposing to harsh environment.
[64]	Planar monopole	Kapton polyimide	Inkjet	Flexible Wireless Devices at 1.2-3.4 GHz	Lightweight and conformal design. Multiband performance in bent configurations.
[65]	Square patch antenna	NinjaFlex	Prenta Duo 3D - printer.	Wearable antennas and wireless on-body applications. At 2.45GHz	Excellent wireless performance when bent. Good impedance matching and efficiency.
[33]	Meandered-line antenna	paper	Screen-printing	Low-Cost RFID and Sensing Applications	Good radiation efficiency. Acceptable return loss, bandwidth, gain, and radiation pattern for mid and short-range RFID. Flexible and stable thermally and electronically.
[66]	Microstrip patch	Elastomeric polydimethylsiloxane	Soft lithographic process	Conformal antenna applications. At 3-4 GHz	Good performance of the flexible antenna with no hysteretic behavior. New and novel fabrication technique.
[67]	Inverted-F antenna (IFA)	Fabric	Dimatix 2831 printer	Wearable electronics applications at 2.45GHz	Shows an acceptable return loss and radiation pattern. No significant difference between the simulated and fabricated results.
[68]	Microstrip patch	Fabric	Screen-Printed with stretchable silver ink DuPont PE873	Millimetre-wave Applications at 77 GHz band	The antenna array maintains a good performance in flat and bent conditions. The antenna array succeeds in detect moving objects in three different directions.

اونيورسيتي تېكنيكل مليسيا ملاك

UNIVERSITI TEKNIKAL MALAYSIA MELAKA

Sashmitha et al. demonstrates a flexible antenna prototype for 5G applications using inkjet printing with silver nanoparticle ink as in Figure 2.1 achieved a high gain of 11.43 dBi at 45 GHz with a bandwidth of 26-40 GHz. The process regarding a set of stages to enhance the performance of a printed antenna. First, a print head sprays ink horizontally on a PET substrate mounted on a platen whose temperature is maintained at 28°C to ensure ink setting. The temperature of the print head is adjusted to match the wetting behaviour of the ink to ensure that it wets the substrate in the right manner. Finally, the antenna is printed and then baked at 150°C for 30 minutes to ensure that the epoxy has set properly. This high-temperature treatment enhances the conductivity of the printed antenna since it is assumed that the solvent in the ink evaporates and the ink particles adhere to each other to enhance conductivity. Baking also reduces the return loss of the antenna, which is the power lost due to mismatching, and indicates better matching and, therefore, better performance [12].

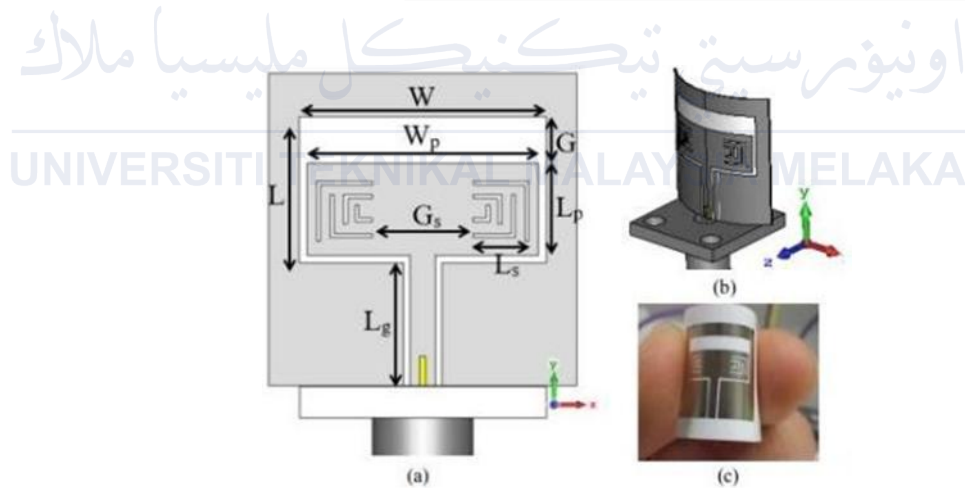


Figure 2.1: PET film with a flexible inkjet-printed antenna [12]

2.4 Analyzing several techniques for designing advanced antennas to improve performance and flexibility.

Abbasi et al. analyzed the impact of the width and length of squares of a wired metal mesh on a special type of MIMO antenna that has closely placed elements. The findings are depicted in Figure 2.2 below and the summary in Table 2.4 below, which sought to determine the optimum size of the mesh square, which meets the requirements of transparency, resonance frequency, impedance matching, and isolation. This optimization is essential for enabling the operation of the MIMO antenna as desired while making it unobtrusive and adaptable [3].

Table 2.4: Parametric analysis of the MIMO antenna [3]

l (mm)	w (mm)	O.T (%)	Frequency (GHz)	S_{11} (dB)	S_{12} (dB)
1	0.1	83	4.63	-28	-19.5
1	0.2	69	4.72	-11	-24
1	0.3	59	4.88	-15	-17
2	0.1	91	4.27	-12	-20
2	0.2	83	4.5	-22	-19
2	0.3	76	4.55	-34	-16
3	0.1	94	4.26	-7	-13
3	0.2	88	4.28	-15	-10
3	0.3	83	4.3	-15	-11

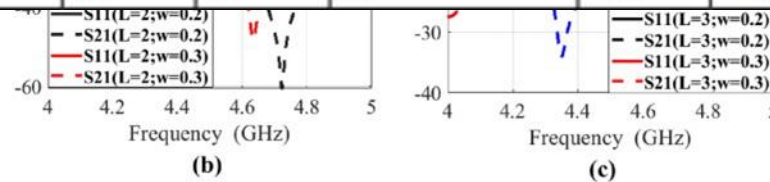


Figure 2.2: Parametric analysis for metal mesh lattice size of the proposed transparent and flexible MIMO antenna (a) $l = 1$ mm, $w = 0.1$ to 0.3 mm, (b) $l = 2$ mm, $w = 0.1$ to 0.3 mm, (c) $l = 3$ mm, $w = 0.1$ to 0.3 mm [3]

The definition of optical transparency (O.T) for a square lattice of a wired metal mesh can be defined by the formula: -

$$O.T = \left[\frac{l}{w+l} \right]^2$$

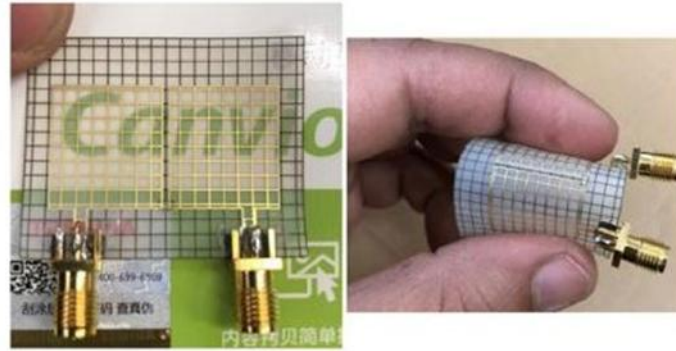
The analysis results show that the proposed structure has a better value of OT when the size of the squares is increased (l), and the width of the wires is decreased (w). This is because less copper area is less opaque and denies less light passing through it than more copper area. However, this improvement in OT comes at a certain cost. Decreasing the amount of copper probably reduces its radiation performance, that is, signal transmission and reception efficiency. Thus, the design of the antenna implies the definition of the size of the squares (l) and the width of the wires (w) to be as small as possible to obtain good optical transparency and, at the same time, the radiation performance of the antenna is satisfactory. This balancing act is tricky, especially for MIMO antennas with closely located antenna elements.

Changing the values of (w) and (l) also changes the resonance frequency of the individual antenna elements as shown in Table 2.4. To obtain the specific resonance frequency, fine-tuning of these parameters is required. Another problem is ensuring that the values of (w) and (l) are precisely managed to achieve the right resonance frequency. These equations show that by increasing the value of (l), the resonance frequency can decrease, while increasing (w) may lead to an increase in the resonance frequency. Thus, achieving an appropriate balance is important.

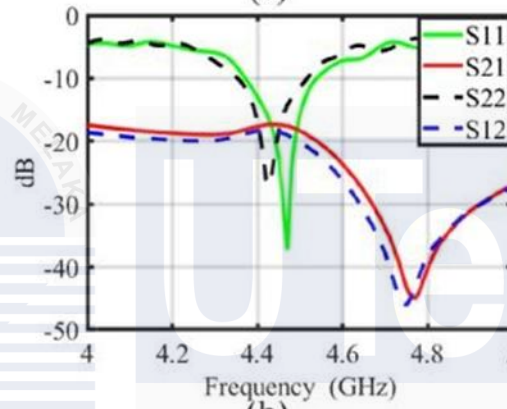
The (w) and the (l) parameters also have a direct influence on the impedance matching of each of the antenna elements. It is also identified that the impedance matching of the MIMO antenna elements is a function of the square lattice parameters and has a random behavior with the change in the parameters. Hence, the fine-tuning of both the (w) and (l) parameters is also necessary to obtain the correct degree of impedance matching besides the necessary optical transparency.

Coupling between the antenna elements is also influenced by the wire width (w) and the square size (l). These dimensions have to be chosen in such a way that it provides good isolation in the sense that no element can interfere with the other. The case is similar to the analysis, in which it was concluded that as w and l are increased, isolation decreases. Thus, fine-tuning is essential to achieve the maximum isolation levels while keeping other performance characteristics in mind. This analysis assists in determining the optimal value for w and l the chosen dimensions are $l = 2$ mm and $w = 0.2$ mm, and offer the highest transmission (83%), signal capture (return loss of 22 dB) and low interference (isolation of 19 dB) at 4.5 GHz for this transparent and flexible MIMO antenna design with closely spaced elements.

Manufacturing and testing have approved the simulated performance of the suggested transparent and flexible MIMO antenna. Figure 2.3(a) shows the developed prototype, while Figure 2.3(b) displays measured scattering parameters. The results obtained from this investigation indicate a good correlation between the measured and simulated scattering parameters. However, these antennas have minor variations in the resonant frequency and transmission coefficient curves. These differences can be due to slight errors in simulation or measurement conditions and imperfect soldered joints. Finally, pattern analysis is used to evaluate the performance of a proposed transparent MIMO antenna for its Envelope Correlation Coefficient (ECC), Channel Capacity Loss (CCL), Total Active Reflection Coefficient, Mean Effective Gain (MEG), and other characteristics that may affect its functionality in most cases.



(a)

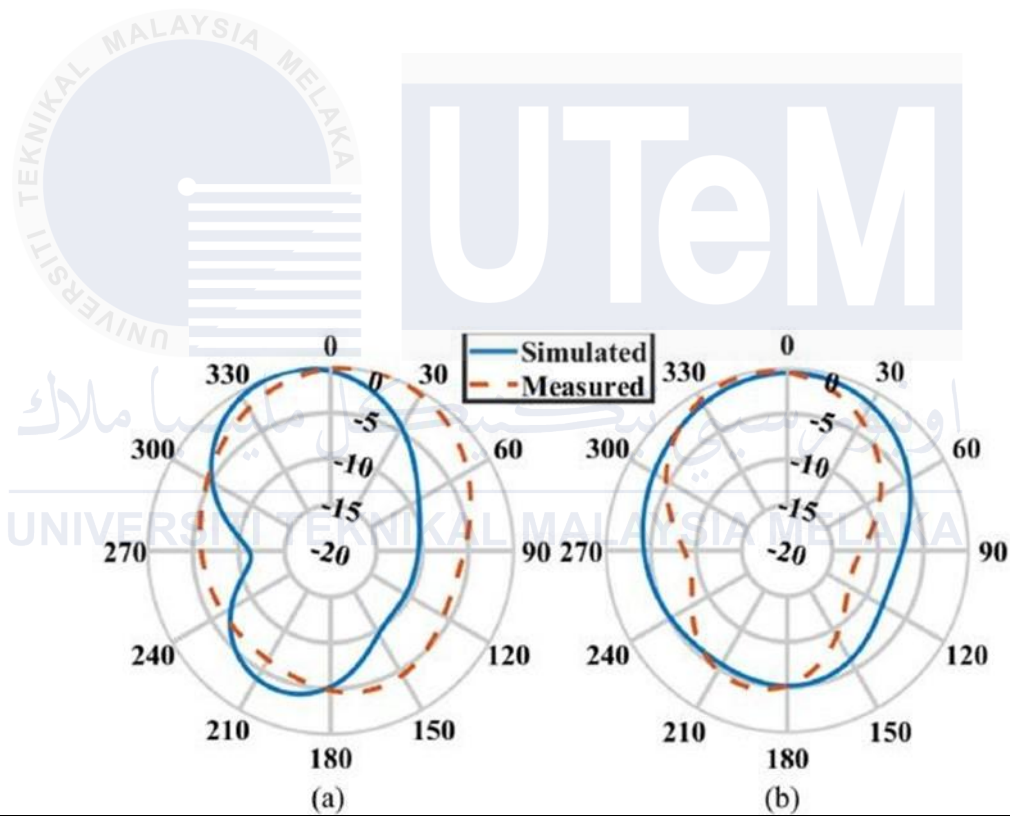


(b)

Figure 2.3: (a) Fabricated prototype of the proposed transparent MIMO antenna, (b) measured scattering parameters for the proposed transparent and flexible MIMO antenna [3]

Figure 2.4 demonstrates the simulated and measured radiation patterns in two orthogonal planes at 4.5 GHz for one of the elements of the transparent patch antenna by using the formula in Table 2.5.

Table 2.5: Formula used by Abbasi et al. [3]



Equation to compute ECC using S- parameters.	$\rho = \frac{ S_{11}S_{12} + S_{21}S_{22} ^2}{(1 - (S_{11} ^2 + S_{21} ^2))(1 - (S_{22} ^2 + S_{12} ^2))}$
Others ECC calculation	$\rho_e = \frac{ \iint_{4\pi} [\mathbf{E}_1(\theta, \phi) \cdot \mathbf{E}_2(\theta, \phi) d\Omega] ^2}{\iint_{4\pi} \mathbf{E}_1(\theta, \phi) ^2 d\Omega \iint_{4\pi} \mathbf{E}_2(\theta, \phi) ^2 d\Omega}$

The product of the two electric fields on the numerator	$\mathbf{E}_1(\theta, \phi) \cdot \mathbf{E}_2(\theta, \phi) = E_{\theta 1}(\theta, \phi)E_{\theta 2}^*(\theta, \phi) + E_{\phi 1}(\theta, \phi)E_{\phi 2}^*(\theta, \phi)$
Calculation the diversity gain of a MIMO antennas	$\text{Diversity Gain}(DG) = 10 \times \sqrt{1 - ECC ^2}$

The element of transparent patch antenna has good radiative performance in Figure 2.4 (a gain of 3.2 dB, radiation efficiency of 61%, and total efficiency of 63%) at this frequency, which is a very good parameter for a flexible and see-through material. Another slightly separated second element shows a similar radiative performance to that described above. Envelope correlation coefficient (ECC) and diversity gain (DG) The Envelope Correlation Coefficient (ECC) is used to measure the correlation between antenna elements

Figure 2.4: Radiation pattern of the transparent MIMO antenna at 4.5 GHz (a) E-plane, (b) H-plane [3]

in a MIMO Diversity System due to coupling amongst them. Lower values of ECC indicate better diversity gains with DG values < 0.517 . ECC can be determined using scattering parameters or far-field patterns for a MIMO antenna.

Figure 2.5 illustrates the ECC and diversity gain performance of the proposed transparent and flexible MIMO antenna employing scattering parameters.

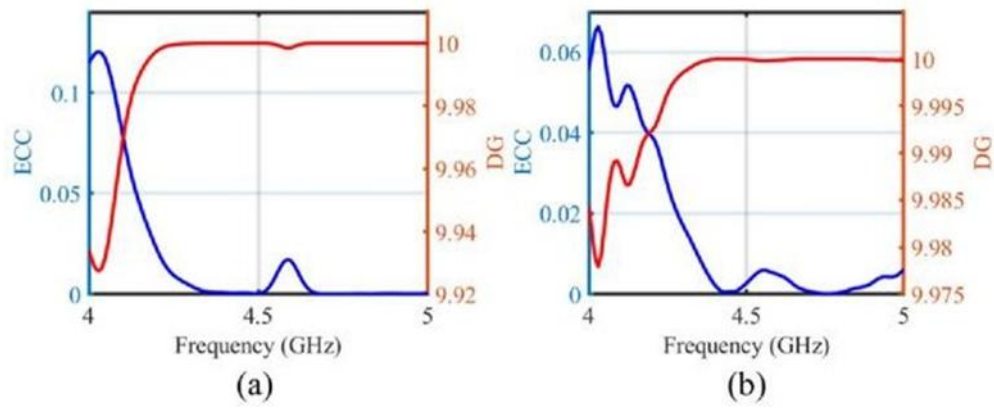


Figure 2.5: The ECC and DG performance of the transparent and flexible MIMO antenna (a) simulated, (b) measured [3]

The antenna achieves an ECC value of 0.005 and a matching diversity gain value of 10 in the intended operating frequency band. The ECC is determined by analyzing far-field patterns. At a frequency of 4.5 GHz, the ECC value is 0.107 as shown in Figure 2.5. At the centre frequency and extreme frequencies of the frequency band, which have an impedance bandwidth of -10 dB, the ECC values are 0.157 at 4.41 GHz and 0.163 at 5.56 GHz, respectively. The ECC values are marginally greater than those derived from scattering parameters. Nevertheless, these values are still significantly lower than the minimal threshold of 0.5 necessary for ECC.

Table 2.6 compares the proposed work with similar studies done in the past. From the analysis, it is clear that the novel transparent and flexible MIMO antenna proposed in this paper, with the antenna elements placed very close to each other, performs as well as

Ref. no	Freq. bands (GHz)	Substrate	Conductor	Element spacing (mm)	Flexibility	O.T (%)	Isolation (dB)	Peak gain (dBi)	Radiation eff. (%)
¹⁵	4.4–5	PET	Ni-metallic mesh	5	Yes	91	20	3.8	85
¹⁶	2.21–6	Melinex	AgHT-4	11.08	Yes	70	15	0.53	41
This work	4.41–4.56	PET	Wired metal mesh	0.9	Yes	83	19	3.2	61

Table 2.6: Comparison with previous recent works [3]

similar works, perhaps even better, given that the spacing between the antenna elements is much smaller in the proposed design.

Meanwhile, Sashmitha et al. planned a flexible antenna then sculpted and parametrically used in the HFSS software before becoming printed with inkjet printing. Experiments and parameters are used to validate simulated results. Near-field scanning is used to examine an antenna's radiation properties, and the results are used to calculate antenna gain. The measured and simulated bandwidths, E and H plane radiation plots, and antenna peak gain are a function of different frequencies [12].

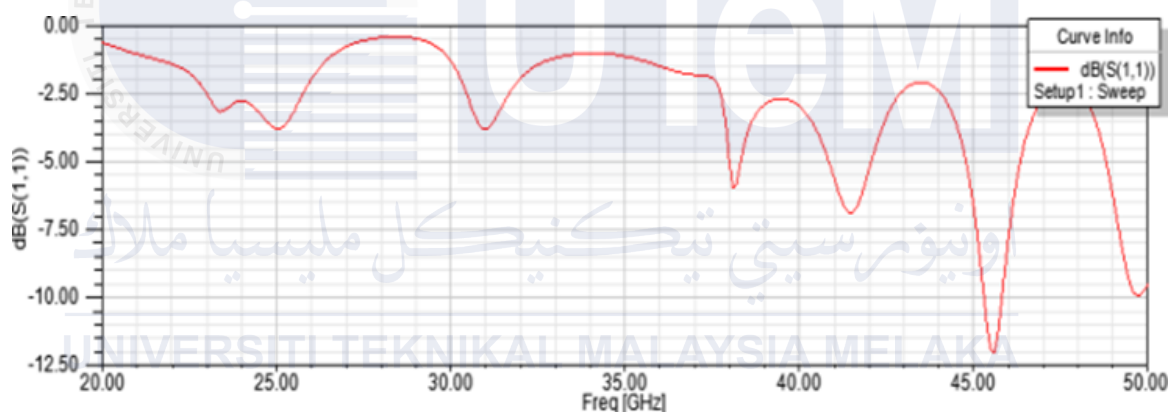


Figure 2.6: The S11 plot of the PET film flexible inkjet-printed antenna [12]

Figure 2.6 shows the simulated and measured S11 plots of the millimeter wave inkjet-printed antennas with the operating bandwidth between 26-40 GHz and includes uniformity deviations in the simulation. This means that the antenna is well-suited for operation when it is compacted. S11 rises notably because of the conductivity enhanced by warmth-sintered metal and the chemically self-sintered layer. If validation is done poorly, then mismatches and minor shifts are obtained.

The reflection coefficient of the proposed mm-wave flexible antenna is depicted in Figure 2.7 as Plots with ringed and brave lines. E and H plane cuts to produce a reflection

coefficient pattern at various impedance bandwidth frequencies. The observed values could have a similar radiation profile to the models.



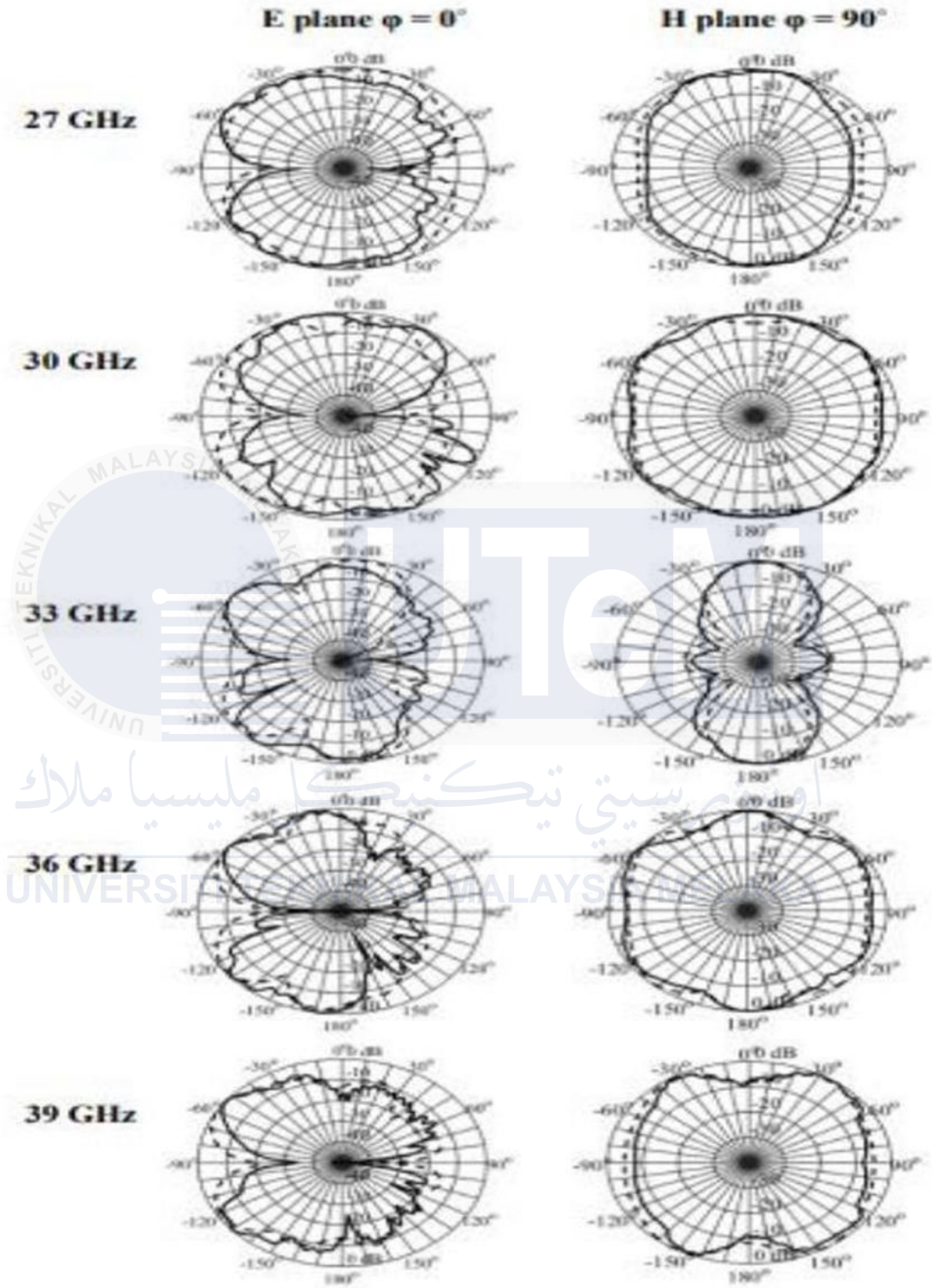


Figure 2.7: Simulated and measured normalized radiation patterns of the flexible inkjet printer antenna at distinct frequencies of the operating range antenna [12]

The realized gain of the proposed mm-wave flexible antenna at various frequencies is presented in Table 6. Initial peak gain estimates from simulations were validated by testing the antenna prototype. Two methods were used for gain calculations. Both simulations and measurements are in close agreement, with a peak measured gain of 7.44 dBi at 37 GHz.

Table 2.7: Peak Antenna Gain of an Inkjet-Printed Antenna [12]

Frequency (GHz)	f = 27	F = 34	f = 38	f = 42	f = 46
Gain	2.47	2.53	5.49	6.82	11.94
Measured Gain	1.79	1.52	4.53	6.43	11.43

Based on this research, the result obtained from their study Muhammad Nawaz Abbasi's research in 2023 focused on optimizing the square mesh size of a MIMO antenna for improved performance in terms of transparency, resonance frequency, impedance matching, and isolation. On the other hand, J. Sashmitha's research in the same year centered on the performance evaluation of an inkjet-printed antenna, achieving a peak gain of 7.44 dBi at 37 GHz with an operating bandwidth between 26-40 GHz. Both studies utilized different methodologies and approaches to enhance antenna performance in their focus areas.

Meanwhile, Islam et al. explored the performance enhancements of microstrip patch antennas using defected ground structures (DGS). Their design focused on improving narrowband performance for biomedical applications, specifically in the ISM band. The optimized antenna resonated at 2.45 GHz with a return loss of approximately -30 dB shown in Figure 2.8, achieving a -10 dB impedance bandwidth of 20 MHz (2.442–2.462 GHz). This design achieved a peak realized gain of 7.04 dBi with a total efficiency increase of 17.63% by incorporating DGS [13].

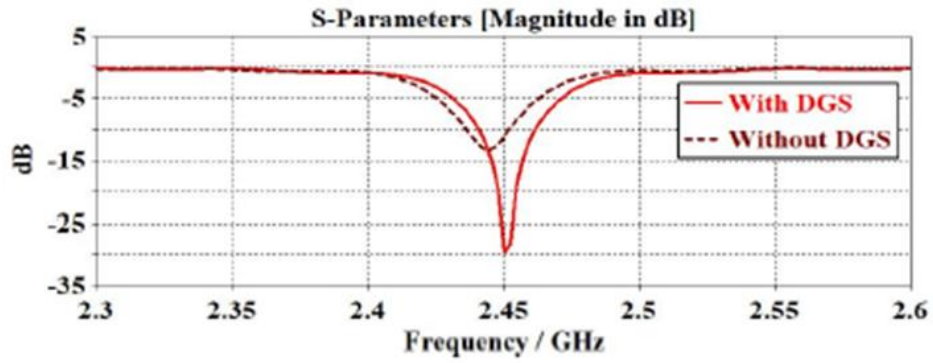


Figure 2.8: S-parameter of the antenna with and without DGS at the resonant frequency [13]

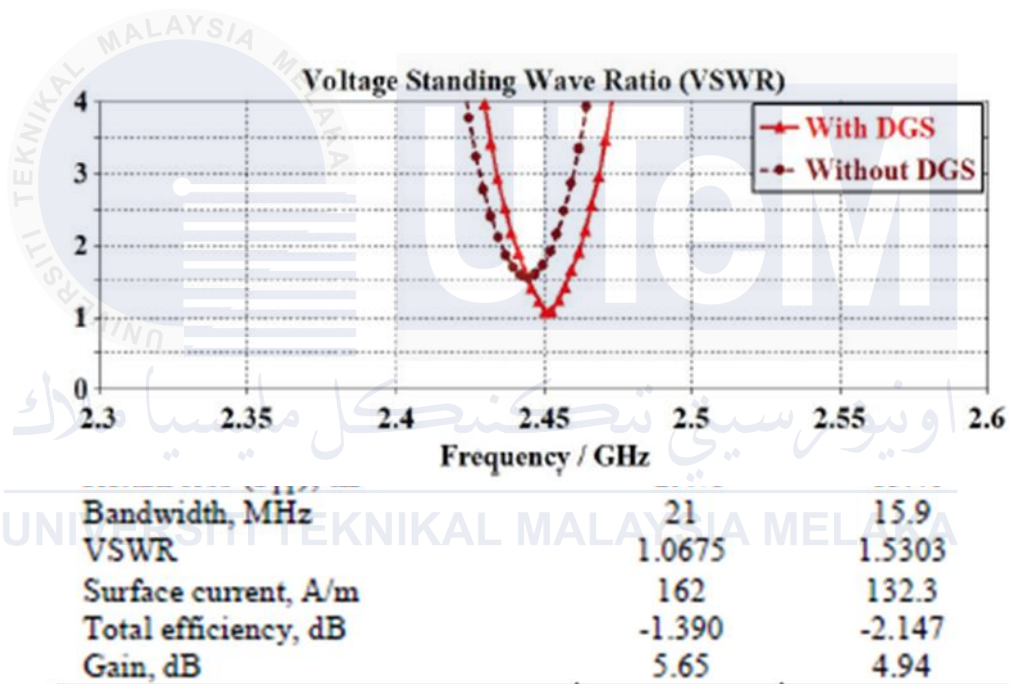


Figure 2.9: VSWR of the proposed antenna [13]

Table 2.8: Comparison table improvement of the antenna with and without DGS [13]

Table 2.9: Comparison table of the antenna to benchmark with existing work [13]

[4]	2.4	- 26.01	78	3.049
[5]	2.45	- 21.19	117	2.80
[6]	2.45	- 18	40	3.9
[11]	2.45	- 26.9	140	3.56
[12]	2.47	- 22.35	70	1.5
This work	2.45	- 29.73	20	7.04

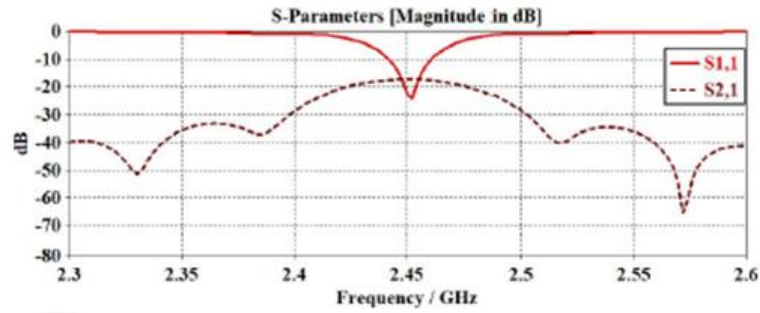
The analysis of the antenna arrays presented in Figure 2.10 reveals a highly efficient performance, with a return loss reaching as low as -25 dB. Notably, there are no observable changes in the bandwidth, which indicates the stability of the antenna's frequency range despite array scaling. The mutual coupling effects between adjacent antennas in the arrays demonstrate commendable isolation, with an S_{21} value around -17.5 dB for the 1x2 array. This isolation remains consistent across the larger arrays, including the 1x4 and 1x8 configurations, as indicated in the same figure.

In Figure 2.10, the maximum realized gain over the frequency range is illustrated, showing a significant enhancement as the array size increases. Specifically, the realized gains for the 1x2, 1x4, and 1x8 arrays are approximately 8 dB, 11 dB, and 13 dB, respectively. This consistent gain improvement underscores the scalability and efficiency of the proposed design for antenna arrays.

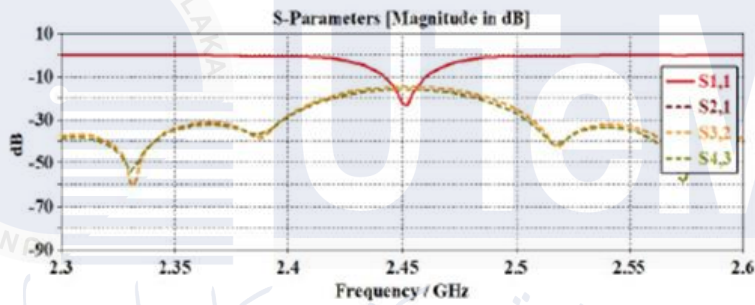
Further, Figure 2.10 highlights that the main lobe direction persists in the boresight direction for all configurations, indicating maintained directional integrity. The directivity gain is notably enhanced with array size, measured at 9.17 dBi for the 1x2 array, 11.7 dBi for the 1x4 array, and an impressive 14.5 dBi for the 1x8 array.

These results conclusively demonstrate that the proposed inset-fed microstrip patch antenna with a defected ground structure (DGS) performs exceptionally well as part of a linear array which is a MIMO antenna. The consistent improvement in gain and directivity

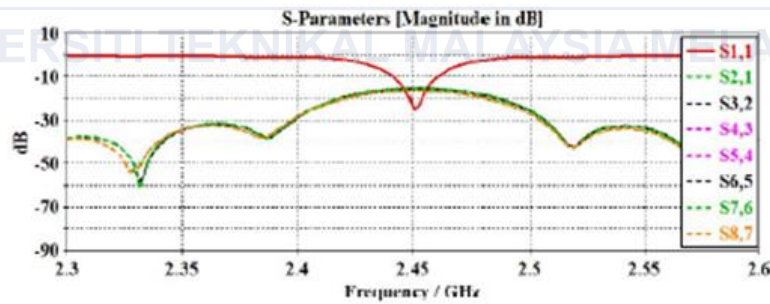
with increasing array size validates the design's adaptability and effectiveness in high-performance applications.



(a)



(b)



(c)

Figure 2.10: S-parameter of the linear array, (a) 1x2 array, (b) 1x4 array, (c) 1x8 array [13]

The formulae utilized by the researchers to derive the parameters for their antenna design which help them in producing the result above are as in Figure 2.11.

Calculation of Patch width (W_p)

$$W_p = \frac{c}{2 f_r \sqrt{\frac{(\epsilon_r + 1)}{2}}} \quad (1)$$

Calculation of Patch length (L_p) -

$$\epsilon_{eff} = \frac{\epsilon_r + 1}{2} + \frac{\epsilon_r - 1}{2} \left[1 + 12 \frac{h}{W_p} \right]^{-\frac{1}{2}} \quad (2)$$

$$L_{eff} = \frac{c}{2 f_r \sqrt{\epsilon_{eff}}} \quad (3)$$

$$\Delta L = 0.412h \frac{(\epsilon_{eff} + 0.3) \left(\frac{W_p}{h} + 0.264 \right)}{(\epsilon_{eff} - 0.259) \left(\frac{W_p}{h} + 0.8 \right)} \quad (4)$$

$$L_p = L_{eff} - 2\Delta L \quad (5)$$

$$W_f = \frac{7.48 \times h}{e^{\left(\frac{Z_0 \sqrt{\epsilon_r + 1.41}}{87} \right)}} - 1.25 \times t \quad (6)$$

$$y_o = \frac{L_p}{\pi} \cos^{-1} \left(\sqrt{\frac{Z_0}{R_{in}}} \right) \quad (7)$$

$$W_g = 6h + W_p \quad (8)$$

$$L_g = 6h + L_p \quad (9)$$

Figure 2.11: Formula used to calculate parameter [13]

All the formulas provided in the study were meticulously utilized to determine the essential parameters required for designing their desired antenna. This process involved calculating and optimizing the dimensions of critical components such as the radiating patch, feed line, inset, and ground plane. By applying these calculations, the researchers were able to precisely tailor the antenna's design to achieve optimal performance characteristics, ensuring that the dimensions of each element contributed effectively to the overall functionality and efficiency of the antenna.

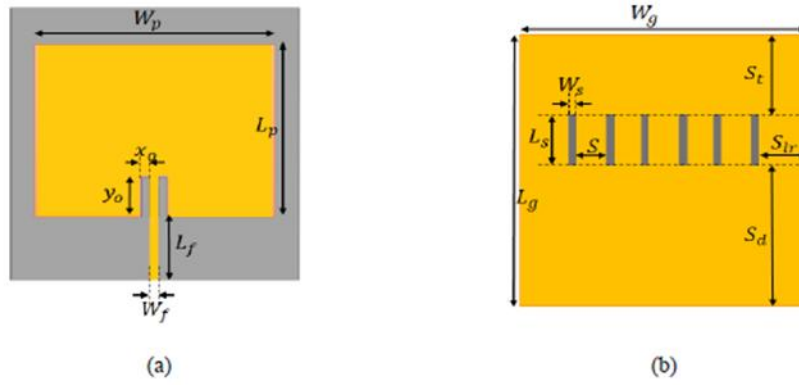


Figure 2.12: Researcher Proposed antenna geometry, (a) top view, (b) ground view [13]

Table 2.10: Physical dimensions of the proposed antenna [13]

Parameters	W_p	L_p	W_f	L_f	x_o	y_o	W_g	L_g	W_s	L_s	S	S_{lr}	S_t	S_d
Dimensions (mm)	46	38	1.41	15	1.41	10	55	60	2	10	6	9.5	21	29

Figure 2.13: The linear antenna array, (a) front view of the 1x2 array, (b) back view of 1x2 array, (c) front view of the 1x4 array, (d) back view of 1x4 array, (e) front view



of the 1x8 array, (f) back view of 1x8 array [13]

Table 2.11: Comparison table of the research paper

Researcher	Muhammad Nawaz Abbasi	J. Sashmitha	Md. Shazzadul Islam
Focus	Impact of square mesh size on MIMO antenna	Inkjet-printed antenna performance	Microstrip patch antenna with defected ground structure
Key Findings	Optimization of mesh square size for transparency, resonance frequency, impedance matching, and isolation	Simulation and measurement of S11 plots, reflection coefficient, radiation patterns, and gain of inkjet-printed antenna	Design and simulation of DGS- based microstrip patch antenna with 20 MHz bandwidth and -30 dB return loss
Results	Improved antenna performance through optimized mesh square size	Peak gain of 7.44 dBi at 37 GHz, operating bandwidth between 26- 40 GHz	Achieved 7.04 dBi gain, 17.63% improved efficiency, VSWR of 1.06
Application	MIMO antenna design optimization	Flexible inkjet- printed antenna design	Biomedical WLAN applications MIMO antenna using a linear array

All three studies present significant advancements in antenna design optimization. Abbasi's work focuses on optimizing transparency and performance balance in MIMO antennas, while Sashmitha's research demonstrates the effectiveness of material enhancements in achieving high gain and broad bandwidth. Islam's contribution adds valuable insights through defective ground structure implementation, achieving precise bandwidth control and improved efficiency for biomedical applications. Together, these studies advance antenna technologies across different aspects from transparency optimization to material innovation and structural improvements contributing to the evolution of modern wireless communication systems in electronic devices.

2.5 Summary

In conclusion, these studies conducted by various brilliant researchers delve into the innovative realm of developing next-generation biomedical antennas using flexible substrates. The chapter showcases a pioneering approach towards designing and modelling MIMO antennas tailored for biomedical applications. The research underscores the importance of meticulous planning in antenna design by emphasizing optimal operating frequencies, materials, and key parameters. Furthermore, the utilization of flexible substrates is highlighted for their ability to enhance patient comfort and adaptability to the body's contours. This chapter also references complementary studies that contribute to antenna design optimization and material advancements, aiming to bolster antenna technologies crucial for modern wireless communication systems. Its comprehensive exploration of antenna design principles and practical applications significantly advances the understanding and potential of flexible substrate-based biomedical antennas in wireless communication and healthcare technology.

CHAPTER 3

METHODOLOGY

3.1 Introduction

The proposed project pioneered the use of flexible substrates for the development of next-generation patch antennas for biomedical applications. It reviews the literature, examines the problem and gaps in the existing literature, and describes how the research proposed in this proposal would advance the body of knowledge about the factors that must be considered to design a proper MIMO antenna. In particular, this work is devoted to designing and modelling biomedical antennas based on flexible substrates. This research recommends improving the effectiveness of MIMO antennas by measuring the antenna output, and the antenna tuning is done using CST Studio Suite. Also, the study explains how this information contributes to the other research sources in the field. When planning to design a MIMO microstrip patch antenna, one has to set the operating frequency, select the appropriate material of the MIMO antenna, and other important factors including VSWR, balance, efficiency, far-field patterns, and S-parameters. This is even more so especially because flexible substrates could be of great value when used in biomedical applications since they can easily be made to fit the shape of the body and are usually less invasive to the patient.

3.2 Selecting and Evaluating Tools for Sustainable Development

During the design and implementation of the MIMO antennas with flexible substrates project, the two most important areas are the choice and evaluation of tools and technologies for data collection and sustainability analysis. This selection process entails methodological

factors such as the accuracy of the antenna simulation software, compatibility of the various materials and testing equipment, and environmental issues of the project. The flexible substrates for fabricating the chosen microfluidics, including PET, LCP and polyimide, must possess flexibility, biocompatibility, and resistance to degradation by wear and tear. However, social and economic concerns are also important in designing the antennas in an affordable way that benefits the patients and healthcare providers. Other crucial activities include performing field tests to compare the performance of the developed antenna under actual conditions, using open-source software to enhance the availability of the developed software, such as CST Studio Suite, and performing life cycle assessments to determine the impacts of the developed antenna on the environment. Thus, the present MIMO antenna for biomedical application project can be successfully completed by carefully selecting and evaluating the tools used in this process, which is crucial for creating efficient, sustainable, and impactful projects that can help develop wearable medical technology and enhance the quality of healthcare services.

3.3 Project flow chart

Biomedical antennas that are designed and implemented on flexible substrates are created in accordance with a well-structured and all-inclusive model for experimentation. At first, a review of the literature was conducted to reveal the current understanding of medical antennas as well as flexible substrates, related issues, and solutions. The choice of flexible substrates included PET, LCP and polyimide due to their flexibility, biocompatibility as well as their ability to withstand rigorous use. During the design of the antenna, the calculation process emphasized the impedance matching, radiation pattern and efficiency of the antenna and CST Studio Suite was used for the simulation of the designs.

After the design phase, the results of simulation and tests were used to determine the potential for improvement, and the use of statistical tools ensured that the data was reliable. Environmental and socioeconomic assessment made the project more sustainable and accessible to the public.

Based on the results, modifications were made to the design as well as the prototypes and re-testing was done to confirm the results. The process was well documented and the results were presented through reports and publications to involve the scientific community and the industry. Project management was made effective through the identification of the right goals, time frame, and the roles to be played. This systematic approach seeks to design effective and durable MIMO antennas employing flexible substrates in wearable medical applications and enhance healthcare services.

The flowchart defines a methodical procedure for the design and analysis of a MIMO (Multiple-Input Multiple-Output) antenna utilizing flexible substrates, segmenting the process into distinct, organized sections. The process commences with a preliminary phase in which the project is suggested, specifying objectives, methods, and anticipated outcomes. A thorough literature survey is conducted to extract ideas from existing research on MIMO antennas and flexible substrates. Based on this basis, an appropriate substrate material is chosen, prioritizing flexibility and durability. A particular antenna design is selected according to the substrate and research findings, and its parameters including dimensions, feed points, and performance characteristics are computed. The design is subsequently modelled and optimized virtually using simulation tools such as CST Studio Suite, which analyzes its radiation pattern, impedance matching, and gain.

The simulation results are assessed to verify if the antenna functions at the specified resonance frequency which is 4.5 GHz. Design parameters are modified as needed, and simulations are conducted again. A parameter sweep is conducted for critical variables such

as width of patch, W_p and length of patch, L_p adjusting the design to provide optimal performance. Upon completion, the design is transformed into a MIMO antenna by the incorporation of numerous antenna elements, which are subsequently simulated and analyzed to evaluate performance parameters, including isolation between elements and diversity gain. The procedure culminates in meticulous recording of the design parameters, simulation data, and findings, offering a detailed record for future reference or publication. This systematic approach guarantees careful consideration of each stage, promoting the creation of a high-performance MIMO antenna utilizing advanced flexible substrates.

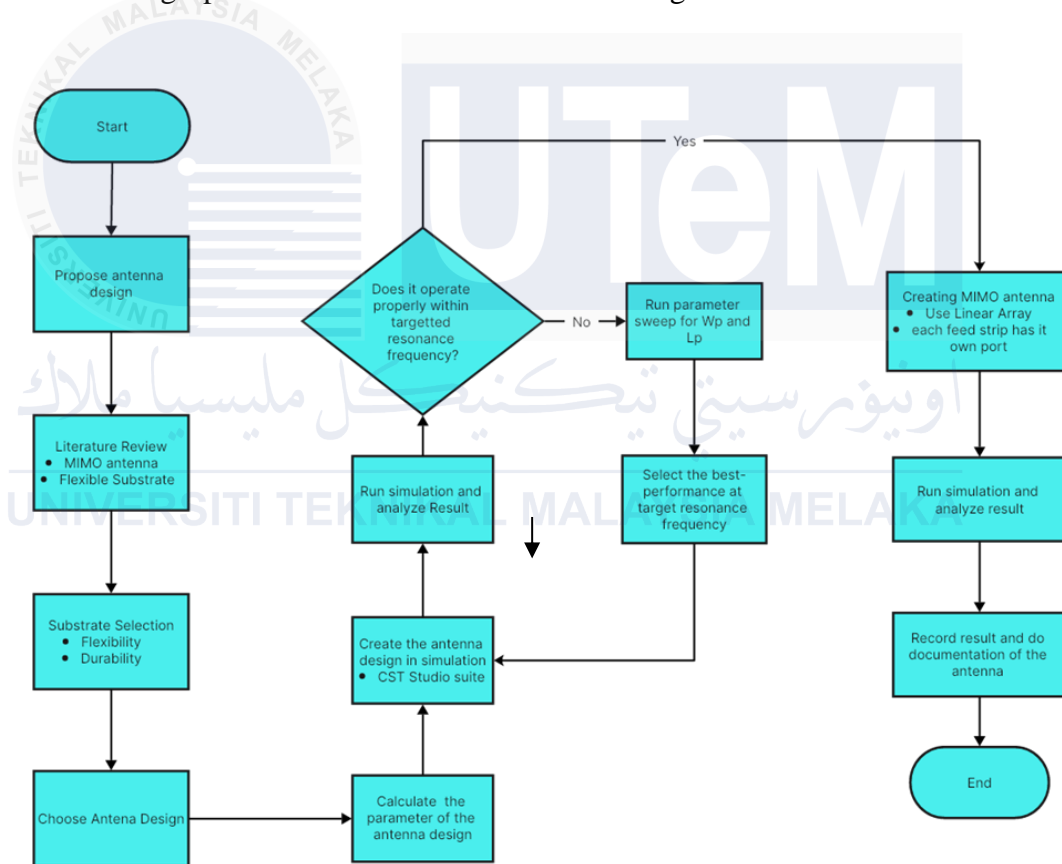


Figure 3.1: Flow chart of Project

3.4 Experimental Setup

The experimental project offers a fresh and holistic approach to the design and assessment of biomedical antennas with flexible substrates. The foundation of the strategy employed in this project is based on flexible electronics and the antenna concept. The chosen method is experimental and quantitative and is designed to design, prototype, and characterize novel high-performance wearable MIMO antennas that operate at resonance frequency 4.5GHz. This involves empirical modelling, simulation, and statistical analysis as the approach. The method is sequentially implemented as selection of material, design of antenna, simulation, and analysis. Figure 3.1 presents an overview of the research design of this thesis. Figure 3.2 provides clear and distinct perspectives of the proposed antenna design. Figure 3.2(a) displays the front aspect of the antenna patch, which is composed of copper. The diagram provides a comprehensive explanation of the patch components involved in constructing the antenna. The substrate used for this particular designed antenna is Polyethylene terephthalate (PET) with a dielectric constant of 3.5. The ground plane's design is clearly illustrated in Figure 3.2(b), which displays the backside with the inscriptions indicating that the ground plane with DGS is composed of copper. Finally, the global perspective view in Figure 3.2(c) shows the design in a three-dimensional view, not only the front side and back side views but the side view of the whole layout and the position of the copper patch and the copper ground plane.

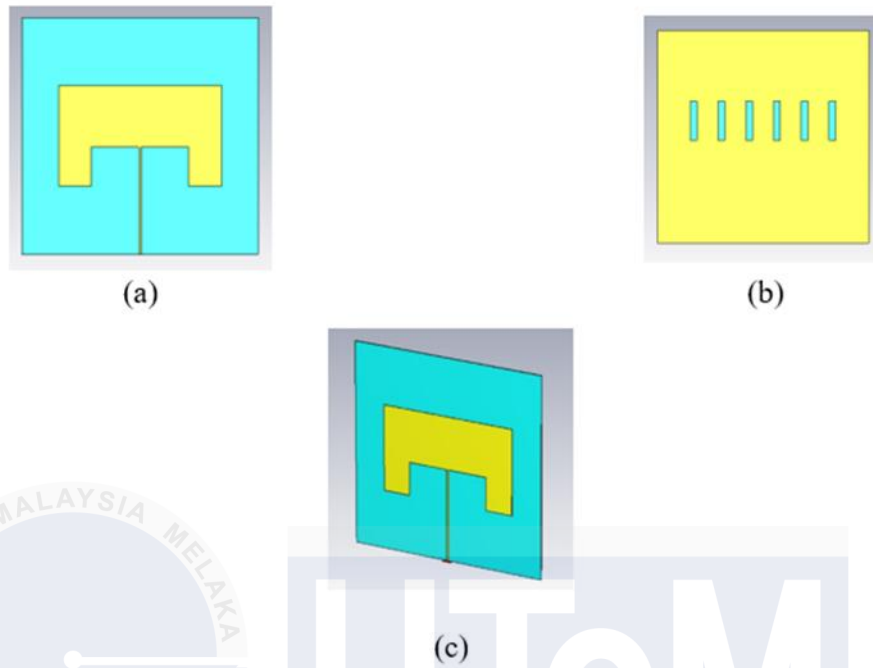


Figure 3.2: (a)Front view of the proposed antenna, (b)Back view, and (c)Perspective view

3.5 Antenna Design

The design and optimization of antenna parameters entail a complex process that integrates theoretical calculations, computer simulations, and simulation result observations. Theoretical models provide the first estimates of essential parameters, including resonant frequency, impedance, radiation pattern, and bandwidth. These models are based on proven electromagnetic principles and assist in the preliminary design of the antenna. Utilizing sophisticated software such as CST Microwave Studio inside the CST Studio Suite helps improve precision by considering intricate antenna shapes, material characteristics, and environmental interactions. These simulations enable the analysis of performance measures like return loss, gain, directivity, efficiency, and far-field patterns in controlled settings. The simulation also offers insights into potential problems such as undesirable resonances, mutual coupling in antenna arrays, or impedance mismatches.

3.5.1 Evaluation of flexible substrates

The flexible substrates and antennas are evaluated through secondary research using the literature review on the flexible substrates that outline the properties of flexible substrates and their suitability in use for biomedical applications as well as searching for other existing designs of MIMO antennas and operation principles and performance characteristics Principles and Performance Characteristics.

3.5.2 Design and Analysis of high-performance Antenna

High-performance biomedical antenna design and analysis using CST Studio Suite The following task is to design and analyze a high-performance biomedical antenna by fully utilizing the powerful electromagnetic simulation software CST Studio Suite. Multiple antenna geometries with different feeding techniques and material properties are explored to deliver the specified performance characteristics, and at various heights, the phantom model also be studied.

3.5.3 Run the simulation and analyze the antenna output

Parametric studies and optimization processes are carried out to fine-tune the characteristics of the antenna. The designed antenna is characterized entirely through full-wave electromagnetic simulations in the CST Studio Suite. Simulated S-parameters, radiation patterns, gain, efficiency, and other pertinent performance parameters will be analyzed. The characteristics of the antenna under different bending conditions and at various heights from phantom models also be studied.

3.5.4 Theoretical Dimension

An essential aspect of antenna design, the resonant frequency specifies the optimal operating frequency of the antenna. Accurate calculations are needed to fit the physical dimensions of this antenna to the 4.5 GHz target frequency. Additional antenna dimensions are derived from the substrate's dielectric characteristics and the speed of light (c). All four of these factors affect the radiation pattern, bandwidth, return loss, and impedance of the antenna.

Polyethylene Terephthalate (PET), which has a dielectric constant (ϵ_r) of 3.5, is used as the substrate material for the microstrip patch antenna. An inset-fed design guarantees effective impedance matching at the antenna's 4.5 GHz resonance frequency. When recalculating the parameters, the material and operation frequency were considered. Patch width (W_p), determined by (1), influences impedance matching and resonance. The patch length (L_p), which is crucial for choosing the resonant frequency, is computed using the fringe effects formula (5), where ϵ_{eff} is the effective dielectric constant.

The characteristic impedance of 50 ohms is attained by optimizing the feedline width (W_f) to facilitate effective signal transmission. To achieve excellent impedance matching and minimize return loss, the inset length (y_o) and width (x_o) are meticulously adjusted typically, the inset width aligns with the feedline width. To ensure adequate support and grounding, the dimensions of the ground plane (W_g and L_g) are adjusted according to formulas (8) and (9), where h represents the substrate thickness which is equal to 0.1mm.

Additionally, the antenna incorporates a Defected Ground Structure (DGS) with optimized slots to enhance gain, bandwidth, and current distribution on the patch. These modifications result in improved antenna performance for the targeted frequency range. The design parameters were further refined and validated using CST Studio Suite, ensuring optimal operation with the PET substrate.

$$W_p = \frac{c}{2f_r \sqrt{\frac{(\epsilon_r + 1)}{2}}} \quad (1)$$

$$W_p = \frac{3 \times 10^8}{2(4.5 \text{ GHz}) \sqrt{\frac{((3.5) + 1)}{2}}}$$

$$W_p = \frac{1}{45} = 0.0222 \text{ m}$$

$$W_p = 22 \text{ mm}$$

$$\epsilon_{eff} = \frac{\epsilon_r + 1}{2} + \frac{\epsilon_r + 1}{2} \left[1 + 12 \frac{h}{W_p} \right]^{-\frac{1}{2}} \quad (2)$$

$$\epsilon_{eff} = \frac{(3.5) + 1}{2} + \frac{(3.5) + 1}{2} \left[1 + 12 \frac{0.1}{22} \right]^{-\frac{1}{2}}$$

$$\epsilon_{eff} = 3.4672$$

$$L_{eff} = \frac{c}{2f_r \sqrt{\epsilon_{eff}}} \quad (3)$$

$$L_{eff} = \frac{3 \times 10^8}{2(4.5 \text{ GHz}) \sqrt{3.4672}}$$

$$L_{eff} = 0.01790149 \text{ m}$$

$$L_{eff} = 17.9015 \text{ mm}$$

$$\Delta L = 0.412h \frac{(\varepsilon_{eff} + 0.3) \left(\frac{W_p}{h} + 0.264 \right)}{(\varepsilon_{eff} - 0.258) \left(\frac{W_p}{h} + 0.8 \right)} \quad (4)$$

$$\Delta L = 0.412(0.1) \left[\frac{((3.4672) + 0.3) \left(\frac{22}{0.1} + 0.264 \right)}{((3.4672) - 0.258) \left(\frac{22}{0.1} + 0.8 \right)} \right]$$

$$\Delta L = 0.0482 \text{ mm}$$

$$L_p = L_{eff} - 2\Delta L \quad (5)$$

$$L_p = 17.9015 - 2(0.0482)$$

$$L_p = 17.8051 \text{ mm}$$

$$L_p \approx 18 \text{ mm}$$

$$W_f = \frac{7.48 \times h}{e^{\left(Z_o \frac{\sqrt{\varepsilon_r + 1.41}}{87} \right)}} - 1.25 \times t \quad (6)$$

assume : $Z_o = 50 \Omega$

$$W_f = \frac{7.48 \times 0.1}{e^{\left((50) \frac{\sqrt{(3.5) + 1.41}}{87} \right)}} - 1.25 \times \left(\frac{1}{4.5 \times 10^9} \right)$$

$$W_f = 0.2093 \text{ mm}$$

$$y_o = 0.3 \times L_p \quad (7)$$

$$y_o = 0.3 \times 18$$

$$y_o = 5.4 \text{ mm}$$

$$W_g = \frac{c}{2f_r} \quad (8)$$

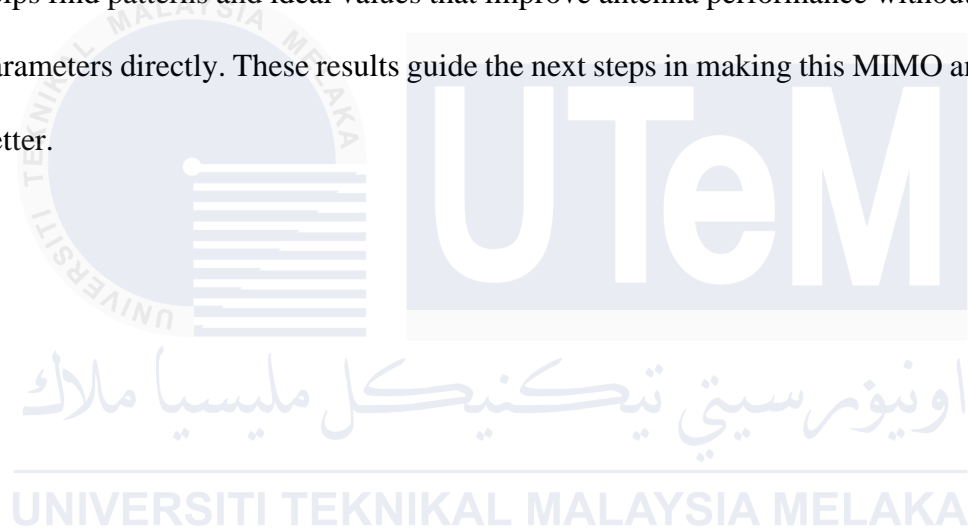
$$W_g = \frac{3 \times 10^8}{2(4.5 \text{ GHz})}$$

$$W_g = \frac{1}{30} = 33 \text{ mm}$$

$$L_g = W_g \quad (9)$$

$$L_g = 33 \text{ mm}$$

These parameters are tested through simulation but it still does not deliver the anticipated antenna performance in the simulation. This issue arose from the neglect of several parameters in the initial computations, which became apparent during the real-world application simulation. That concludes the calculated parameters only serve as a fundamental reference. Thus, parameters sweep is used in CST Studio Suite to optimize the procedure. By changing important factors like W_p , L_p , and W_f , which have a large impact on the results within a certain range, the design can be evaluated methodically. This method helps find patterns and ideal values that improve antenna performance without changing the parameters directly. These results guide the next steps in making this MIMO antenna project better.



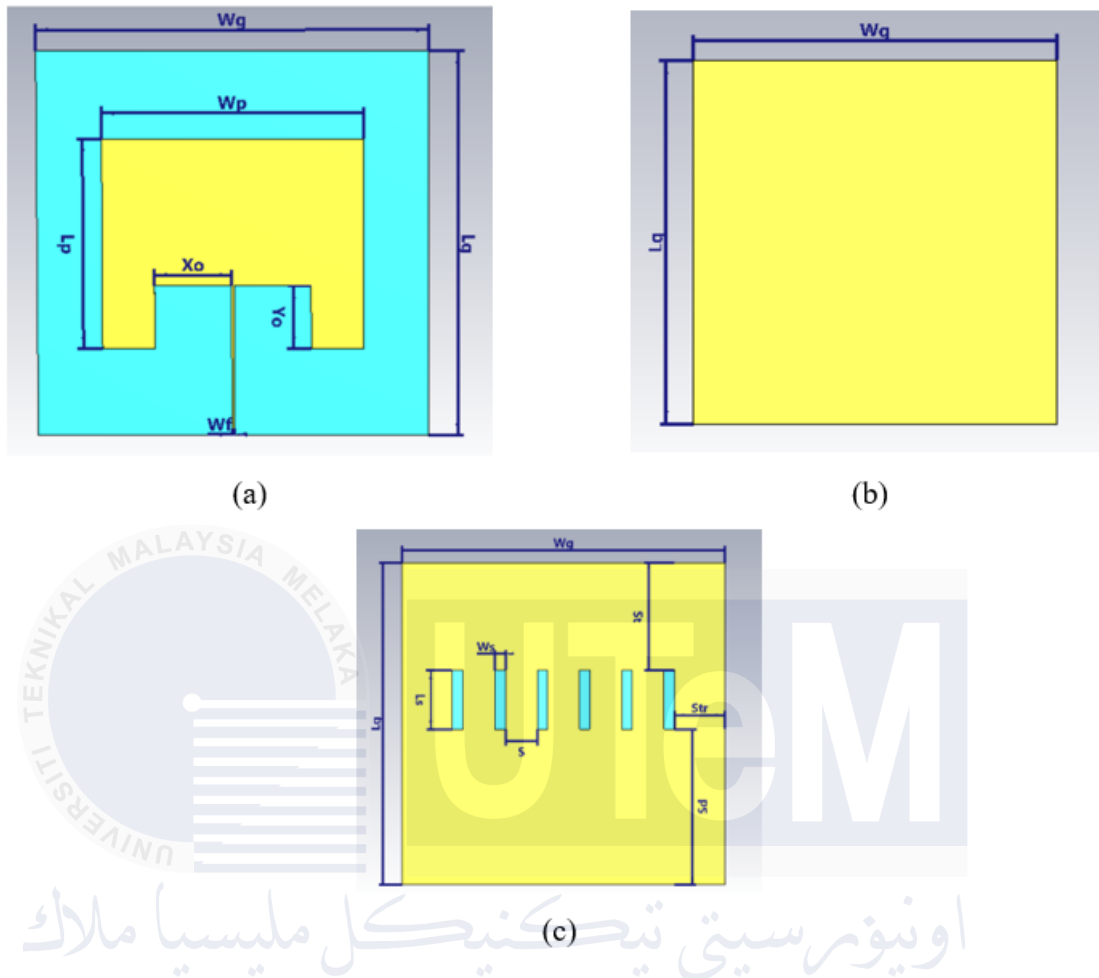


Figure 3.3: (a) Front view (b) Normal Ground (c) DGS Ground (Slot DGS)

3.5.5 Dimensions of the designed antenna after optimization

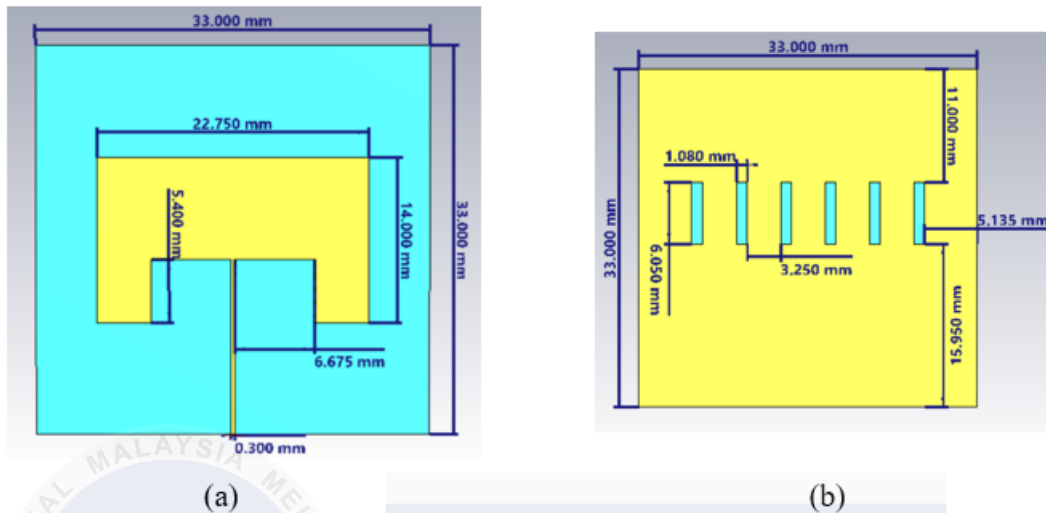


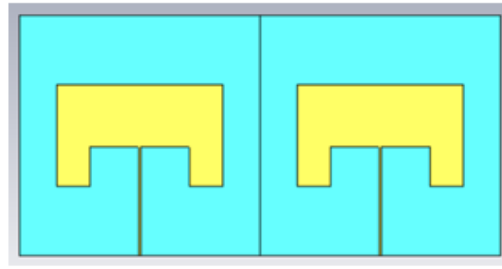
Figure 3.4: Detail parameter of microstrip antenna after the optimization process
(a)Front view (b)Back view

Figure 3.4 shows the optimized microstrip patch antenna with a frequency of 4.5 GHz. The antenna comprises a rectangular patch dimension of 22.75 mm by 14 mm placed on a 0.1 mm thick dielectric substrate. For the current flow, a ground plane of 33 mm by 33 mm is suitable as a reference. The patch is expanded by a 0.3 mm wide microstrip feed line. To improve performance, a defected ground structure (DGS) with a slot shape is used in the ground plane. The 1.08 mm by 6.675 mm DGS is offset 5.135 mm from the ground plane with the edge. The DGS modifies the distribution of current on the ground plane and thus can be used to manipulate the antenna's impedance, bandwidth, and radiation pattern properties. The optimized design defines the desired performance customized to the design requirements at 4.5 GHz, incorporating advancements in bandwidth, side lobe reduction, and gain improvements. Table 3.1 shows the specifications of the antenna dimensions.

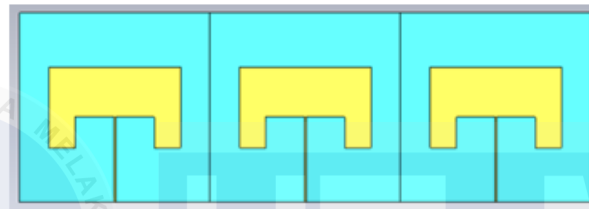
Table 3.1: Parameter of microstrip patch antenna

Parameter List	Value (mm)
W_g	33
L_g	33
W_p	22.75
L_p	14
X_o	6.675
Y_o	5.4
W_f	0.3
h	0.1
W_s	1.08
L_s	5.5
S	3.25
S_t	11.55
S_{lr}	5.135
S_d	15.95

3.6 Designing MIMO antenna



(a)



(b)



(c)

Figure 3.5: (a) 1 x 2 array antenna (b) 1 x 3 array antenna (c) 1 x 4 array antenna

The design process for 4.5 GHz MIMO antennas starts with optimizing the single antenna element. The optimal antenna works on the operational frequency obtained from using sweep parameters such as the dimensions, feed point location, and substrate properties for the individual element to match the desired impedance, bandwidth, and radiation pattern. The optimized element is then used to form the linear array structure in Figure 3.5.

Despite being a simple linear array configuration in nature, the design involves many important parameters which require careful attention. The spacing of the antenna elements is important to get spatial diversity such that each antenna element receives a signal relatively independently. On the other hand, spacing elements can increase mutual coupling, resulting in performance trade-offs. Simulations and parameter sweeps are then used to find the best

element spacing, to maximize spatial diversity without compromising on mutual coupling. In addition to the individual elements, the feeding network that distributes the power to each element in the array also contributes greatly to the performance of the MIMO antenna system.

3.7 Limitation of purposed Methodology

This method of review suffers from many challenges especially when only depending on simulations and not fabricating the microstrip patch antenna. The simulation process was conducted in CST Studio Suite, and several limitations were identified as part of this project.

One of the major tasks was to successfully make the antennas functional at its resonance frequency of 4.5 GHz. In order to achieve this, some compromises had to be made, which led to a poorer return loss when compared to other parameters during the parameter sweep process. This trade-off results in a decrease in the overall efficiency of the antenna which prevents it from working with the lower return loss value at the targeted resonance frequency for practical performances.

Another limitation was the selection of substrate material. The selected material was PET, its low cost as well as good compatibility and resistance, which exhibited minimum return loss at higher resonance frequencies. This affects the performance of the antenna when working on a range of frequencies and might need to tackle more optimization or a choice of different substrates for better performance.

Nevertheless, the results may still be influenced by the computation model's simplifications, the mesh resolution, and the material property approximations, despite

the fact that CST Studio Suite is a sophisticated instrument for antenna design simulation. The simulations likely do not fully represent the interactions between the antenna and its operational environment, such as exposure to various environmental conditions or proximity to biological tissues. Such limitations suggest more accurate simulation models and physical verification studies which lead to more reliable conclusions.

Nonetheless, the methodology proposed still shows consistency for a wide of biomedical antenna modelling processes. This helps in enhancing the practical viability of this approach by adjusting the models with domain experts and best practices to overcome these limitations.

3.8 Summary

The chapter describes the design procedure of high-performance MIMO antennas based on flexible substrates and their biomedical applications. The chapter started with a literature review, highlighting gaps in the existing designs and establishing a need for flexible, biocompatible substrates such as PET, LCP, and polyimide materials. It explained the rigorous and careful process, explaining the substrate selection based on PET, and antenna simulation using CST Studio Suite. Parameters like impedance matching, radiation patterns, and efficiency, were optimized to achieve a resonance frequency of 4.5 GHz. While theoretical modeling and simulation proved successful, there were limits within modeling to be acknowledged, in reality, manufacturing and dynamic performance due to material and environmental limits.

This work also highlighted the advantages of using flexible platforms for biomedical devices, which can be not only more adaptable and even sustainable but also more economical. However, challenges in terms of reduced return loss as well as trade-offs in the

substrate highlighted the need to further refine through additional modeling. This chapter established a strong base for simulation flexible substrate antennas, showing their potential for enhancing healthcare technologies.



CHAPTER 4

RESULTS AND DISCUSSIONS

4.1 Introduction

Multiple Input and Multiple Output (MIMO) antenna technology as an innovative solution to address the issues especially when we want to apply for biomedical application devices. MIMO systems use multiple antennas at both the transmitting and receiving ends, which provides the advantages of spatial diversity & and multiplexing that translates into higher data rate, longer range and less interference. However, it is noteworthy that the incorporation of MIMO antennas in biomedical devices poses challenges such as size, flexibility as well as biocompatibility.

This introduce a new perspective on the conception and development of a MIMO antenna system that is transparent and adaptable for use in biomedical fields. The proposed antenna system for implantable use identifies the crucial problems associated with conformability, biocompatibility, and high-performance communication by using advanced materials and innovative fabrication methods. Employing a low dielectric constant PET substrate, which is flexible, transparent, and made of polyethene terephthalate makes it possible to incorporate the antenna into wearable or implantable systems in addition to having a robust structure and performance.

4.2 Result and analysis by using Theoretical value

The result of the S-Parameter of the antenna by using Theoretical values for parameters is clearly shown in Figure 4.1.

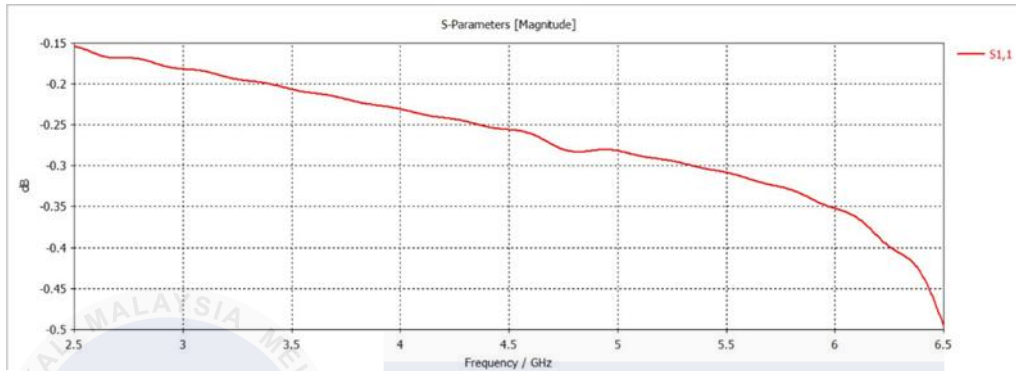


Figure 4.1: Result of S-Parameter from proposed design microstrip antenna (Calculated Parameter)

In designing an antenna to guarantee that the antenna fulfils the predetermined specifications that were established before its development, the simulation results are meticulously examined. The S-parameter results derived from theoretically estimated values are depicted in Figure 4.1. The phenomenon of ‘steep slope’ is observed to impact the return loss value at a frequency higher than the specified resonant frequency of 4.5 GHz. The shortfall in theory that is applied in computation during antenna designing is probably the prime cause of the impedance mismatch. Errors or approximations made in the calculations leading to the physical antenna have a notable influence on the operability of the antenna decreasing the resonance around the targeted frequency.

Since the theoretical parameter didn't achieve the desired result, therefore the optimization process is done as in Figure 4.2 to find the best parameter in which the 'steep slope' happens on the operation frequency.

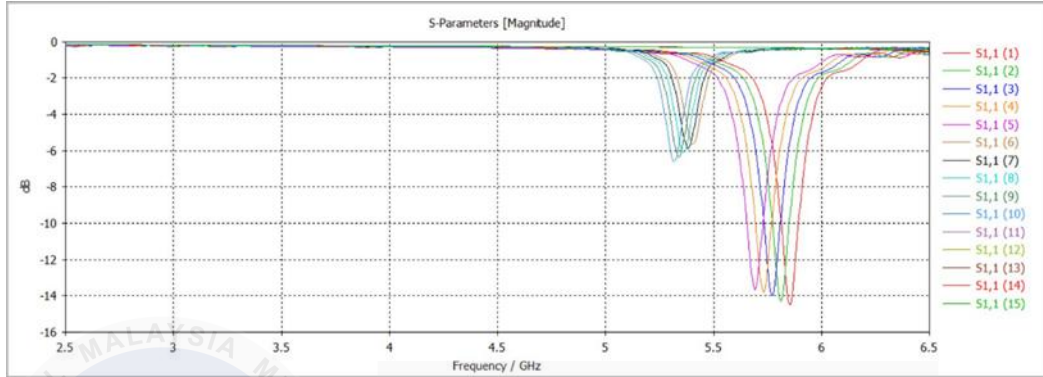


Figure 4.2: Result obtained during parameter sweep

As shown in Figure 4.2 the parameter sweep shows the performance of the antenna in each of the parameters. After analyzing each of the 'slopes' the most suitable and reliable parameter needs to be used when $W_p = 22.75mm$, $L_p = 14mm$ and $W_f = 0.3mm$ because it produces a great impedance matching which makes it work at operation frequency 4.5 GHz after applying DGS.

4.3 Result and analysis of antenna without DGS

The optimized parameter of the selected antenna is then validated through simulation, beginning with the conventional ground antenna, and subsequently observing the performance of the antenna with the implementation of a Defected Ground Structure, DGS. The analysis of the S-parameter without DGS is shown in Figure 4.3.

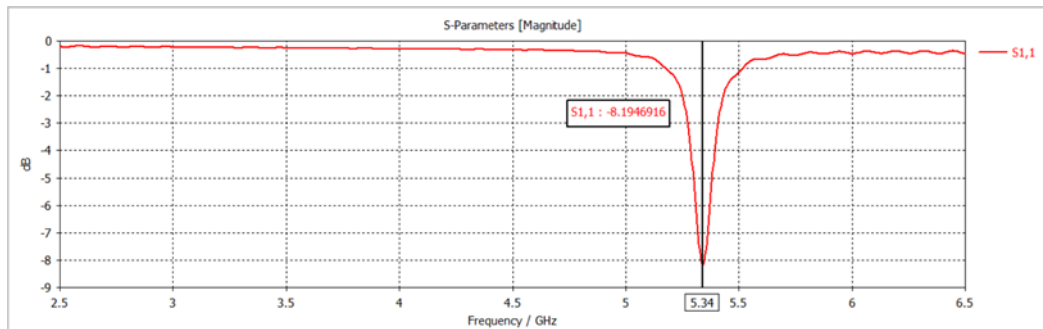


Figure 4.3: S-Parameter analysis to obtain Return Loss

In Figure 4.3 the return loss at -8.19 dB at the operating frequency of 5.3 GHz, which represents a moderate impedance match but far from the resonance frequency chosen which is 4.5GHz.

Figure 4.4 shows the analysis of the bandwidth of the antenna without DGS based on the S-Parameter result.

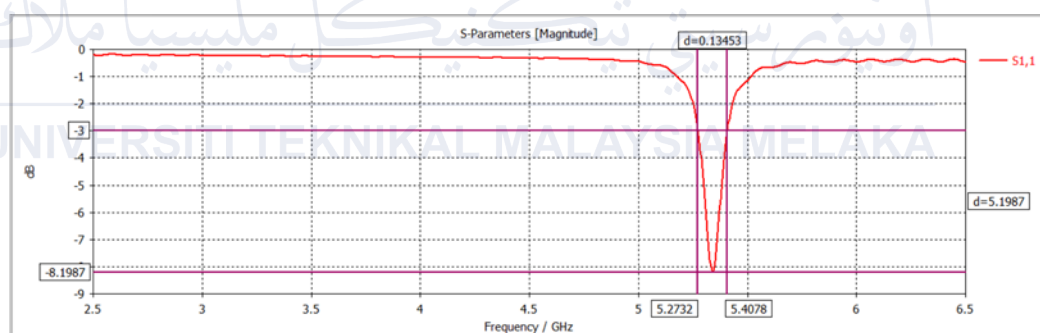


Figure 4.4: S-Parameter analysis to obtain Bandwidth

The S-parameters derived bandwidth shown in Figure 4.4 is wide which is 0.1345 GHz. It indicates a significantly wide operational range makes have lower performance than narrower bandwidth, particularly for biomedical application scenarios.

Figure 4.5 presents the Voltage Standing Wave Ratio (VSWR) characteristics of the antenna, providing insight into its impedance matching and overall performance.

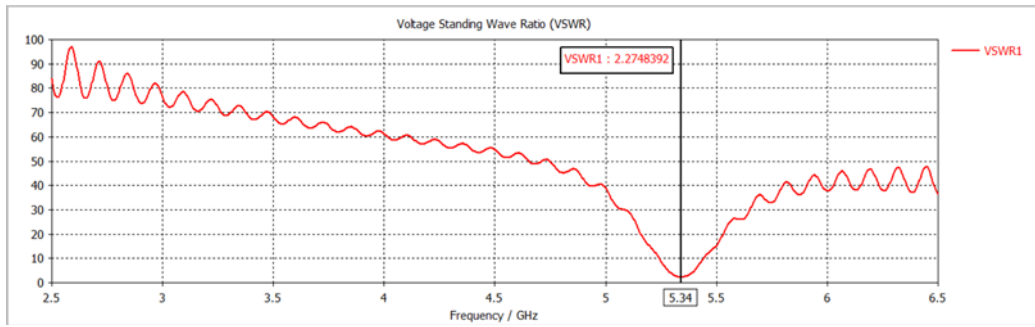


Figure 4.5: VSWR

The VSWR in Figure 4.5 indicates that the VSWR value is 2.27, which is not good, the ideal ratio VSWR is 1:1 but if it is still in the value of $2 \gg VSWR \gg 1$, the antenna can be classified as a ‘Good’ antenna. It can also impact on signal integrity.

Figure 4.6 illustrates the surface current distribution of the antenna throughout the surface area of the antenna.

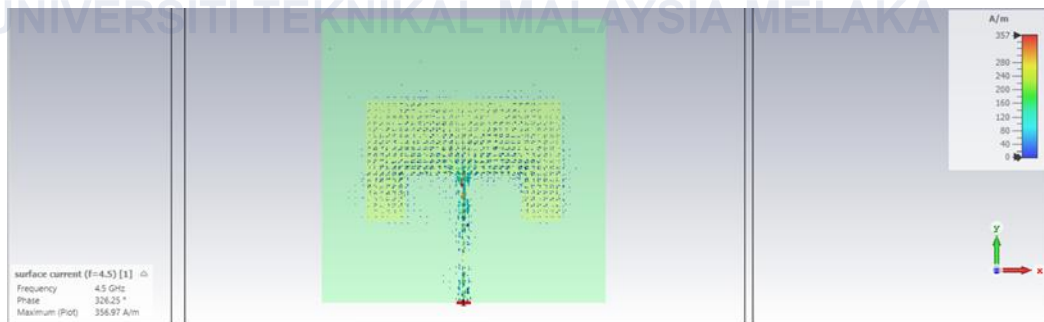
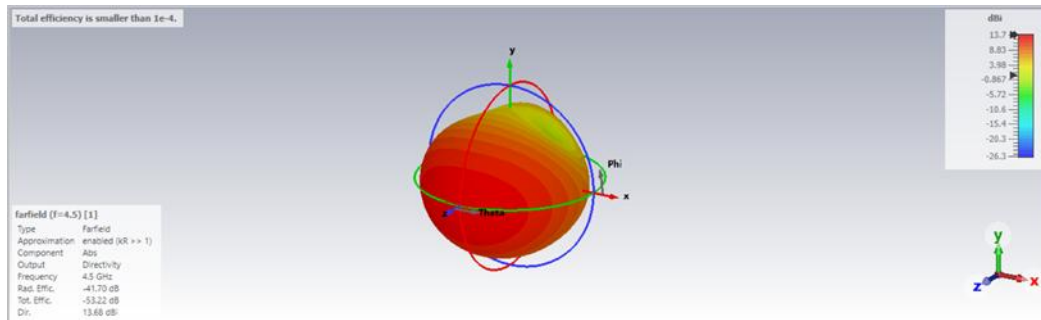


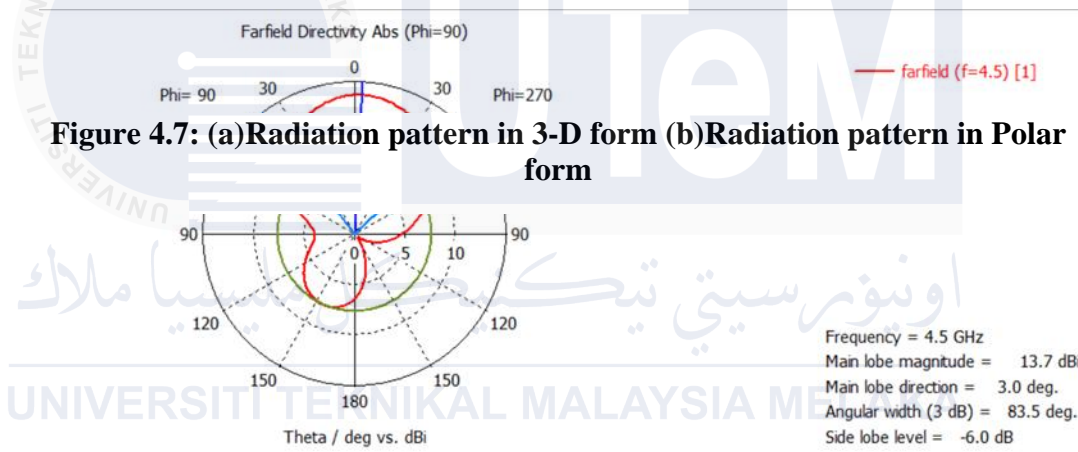
Figure 4.6: Surface current antenna at resonant frequency

Figure 4.6 displays the surface current distribution at resonance, which shows that the antenna conducts current over its surface at the resonant frequency with an efficiency of 356.97 A/m. Important details about the antenna's performance, like its impedance matching and radiation efficiency, are revealed by this distribution.

The antenna's 3D radiation pattern is shown in Figure 4.7 (a), and a thorough perspective of its radiation properties is provided in Figure 4.7 (b), which shows the same pattern in polar form.



(a)



(b)

The antenna's radiation behavior is comprehensively visualized by the 3D radiation pattern in Figure 4.7 (a), which also highlights the antenna's overall efficiency and directional characteristics. This is enhanced by the polar form in Figure 4.7 (b), which makes it simpler to examine the beamwidth, directivity, and symmetry of the antenna by giving a more accurate depiction of the radiation intensity across particular angles. When combined, these visualizations provide insightful information about how well the antenna performs in its intended operating environment. It also shows that the total efficiency is -53.22 dB.

Figure 4.8 illustrates the max gain performance of the antenna across the bandwidth frequency.

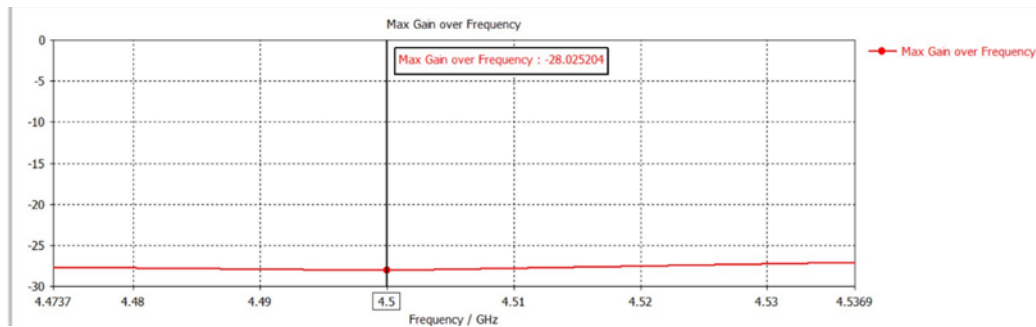


Figure 4.8: Max Gain over frequency for the whole Bandwidth

As seen in Figure 4.8, the highest gain over the bandwidth is noticeably low at -28.03 dBi. This suggests that the antenna's radiation efficiency is low due to large power losses. A low gain rating like this indicates that the antenna might not be able to send or receive signals over long distances or in situations with a lot of interference. For some applications, this can be a major drawback, and more design optimization might be needed to increase the gain and overall performance.

4.4 Result and analysis of antenna with DGS

Figure 4.9 depicts the S-parameter performance of the antenna after the incorporation of a Defected Ground Structure (DGS), highlighting its impact on return loss.

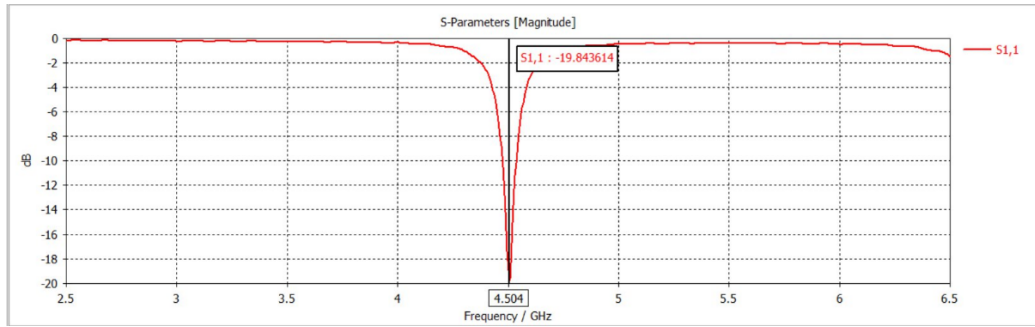


Figure 4.9: S-Parameter analysis to obtain Return Loss

Figure 4.9 illustrates the addition of DGS leads to notable enhancements. Excellent impedance matching at 4.5 GHz is shown by the S-parameter's return loss of -19.84 dB. This enhancement implies that the DGS improves the antenna's capacity to maximize power transfer and reduce signal reflection. These improvements increase the antenna's effectiveness and suitability for its intended use.

Figure 4.10 shows the analysis of the bandwidth of the antenna with DGS based on the S-Parameter result.

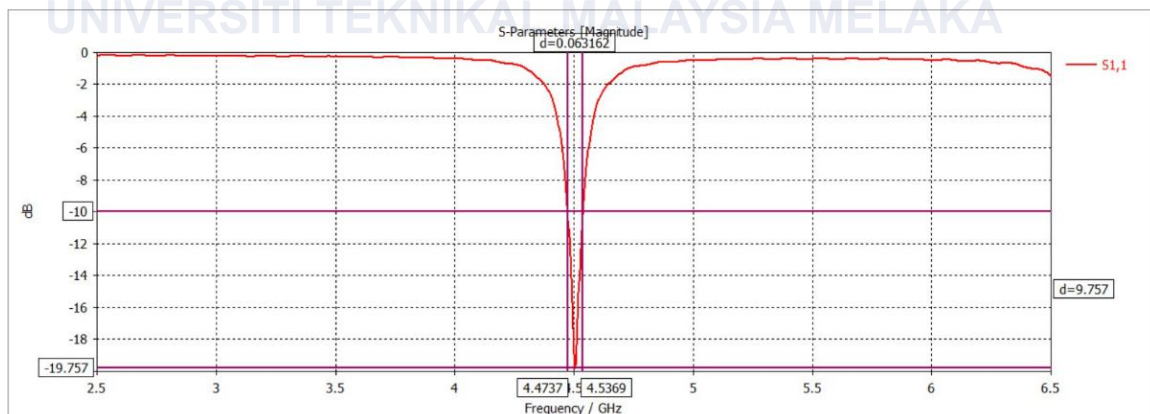


Figure 4.10: S-Parameter analysis to obtain Bandwidth

The S-parameters derived bandwidth shown in Figure 4.10 is wide which is 0.0632 GHz. It indicates a significantly narrower operational range, which has higher performance than a wider bandwidth, particularly for biomedical application scenarios.

Figure 4.11 presents the Voltage Standing Wave Ratio (VSWR) characteristics of the antenna, providing insight into its impedance matching and overall performance for antenna with DGS.

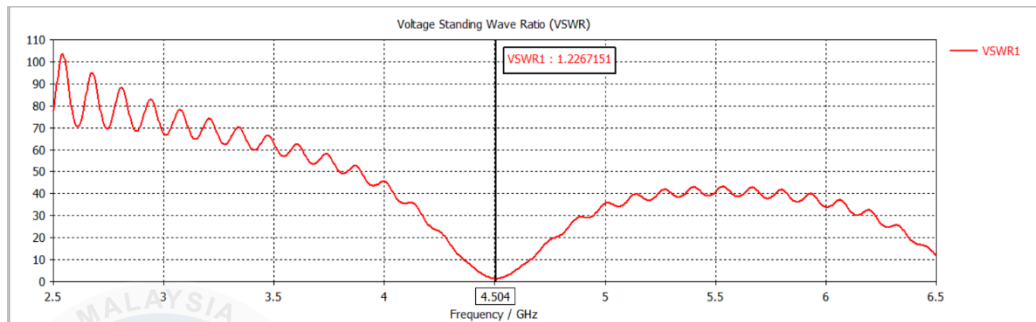


Figure 4.11: VSWR

As can be seen in Figure 4.11, the VSWR much improves to 1.23, which is well inside the acceptable range for best results. This number denotes a small mismatch between the transmission line and the antenna, guaranteeing effective power transfer and little signal reflection. The antenna's overall dependability and efficiency in its operating environment are boosted by the increased VSWR.

Figure 4.12 illustrates the surface current distribution of the antenna throughout the surface area of the antenna with DGS.

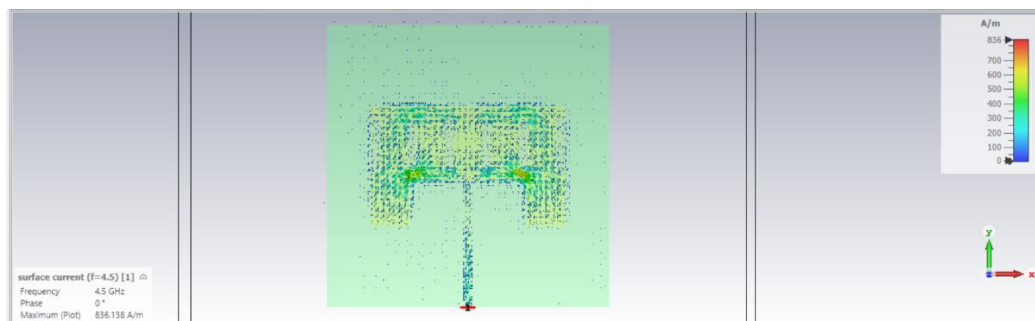


Figure 4.12: Surface current antenna at resonant frequency

Figure 4.12 displays the surface current distribution at resonance, which shows that the antenna conducts current over its surface at the resonant frequency with an efficiency of 836.138 A/m. The value of the current distribution is greatly increased if compared to the result for the antenna without DGS. Effective energy transfer and robust electromagnetic field creation are usually indicated by a higher current density at resonance. Hotspots on the antenna surface can be found using the current distribution pattern, which can also help with design optimization for improved performance and lower losses.

The antenna's 3D radiation pattern is shown in Figure 4.13 (a), and a thorough perspective of its radiation properties is provided in Figure 4.13 (b), which shows the same pattern in polar form.

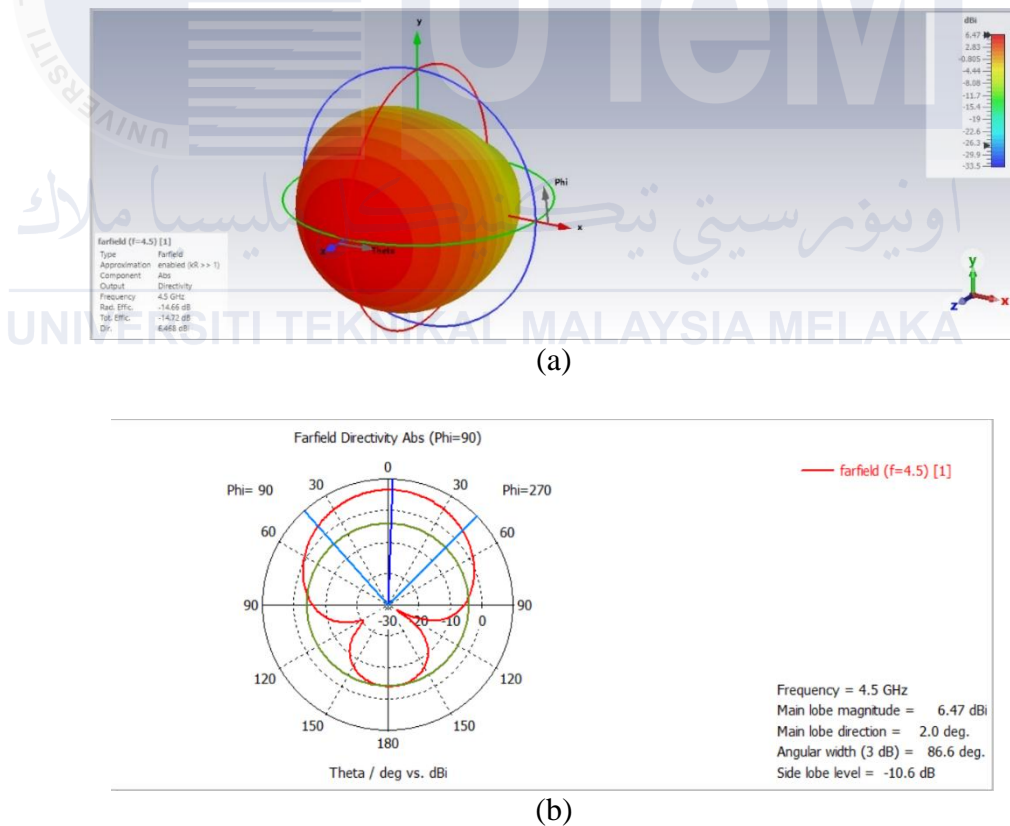


Figure 4.13: (a) Radiation pattern in 3-D form (b) Radiation pattern in Polar form

The antenna's radiation behavior is comprehensively visualized by the 3D radiation pattern in Figure 4.13 (a), which also highlights the antenna's overall efficiency and

directional characteristics. This is enhanced by the polar form in Figure 4.13 (b). It also shows that the total efficiency is increased to -14.72 dB.

Figure 4.14 illustrates the max gain performance of the antenna across the bandwidth frequency.

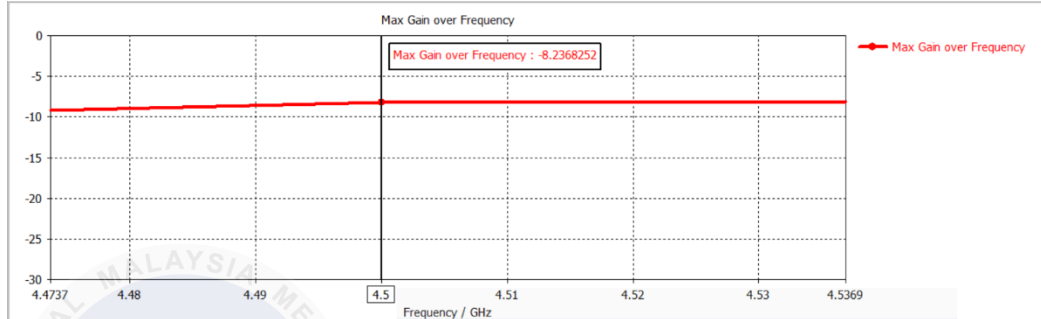


Figure 4.14: Max Gain over frequency for the whole Bandwidth

As seen in Figure 4.14, the highest gain over the bandwidth is noticeably low at -8.24 dBi. This suggests that the antenna's radiation efficiency is high due to low power losses.

Table 4.1: Comparison table of the antenna at the antenna without and with DGS

Name	Without DGS	With DGS
Operation frequency, GHz	5.3	4.5
Return Loss, dB	-8.19	-19.84
Bandwidth, GHz	0.1345	0.0632
VSWR	2.27	1.23
Surface Current, A/m	356.97	836.138
Total efficiency, dB	-53.22	-14.72
Gain, dBi	-28.03	-8.24

4.5 Result and Analysis of MIMO Antenna (Linear Array)

The design incorporates a micropatch antenna configured in a linear array to facilitate MIMO (Multiple-Input Multiple-Output) capabilities, hence improving its gain and directional characteristics. The antenna designs are described in three configurations, 1×2 , 1×3 , and 1×4 arrays. The frontal and posterior views of the structure of 1×3 array antenna are shown in Figures 34(a) and 34 (b), while frontal and posterior views of 1×4 array configuration are represented in Figures 36(a) and 36(b).

The S-parameter results of these antennas, shown in Figures 33, 35, and 38, indicate improved impedance matching and performance. As shown in Figure 4.18, the return loss of the 1×2 array is -22.70 dB (bandwidth is 0.0632 GHz). Not only the return loss has improved to -23.08 dB for the 1×3 arrays shown in Figure 4.20, but the bandwidth is kept stable at 0.16 GHz. Fig. 38 shows the return loss of 1×4 array which demonstrates the return loss of -23.14 dB a bandwidth of 0.16 GHz.

The constant bandwidths across the array configurations demonstrate the scalability of the design while maintaining performance. Larger return loss yield for a larger array size suggests excellent impedance matching, thus these designs can be used in high-performance antennas for biomedical applications.

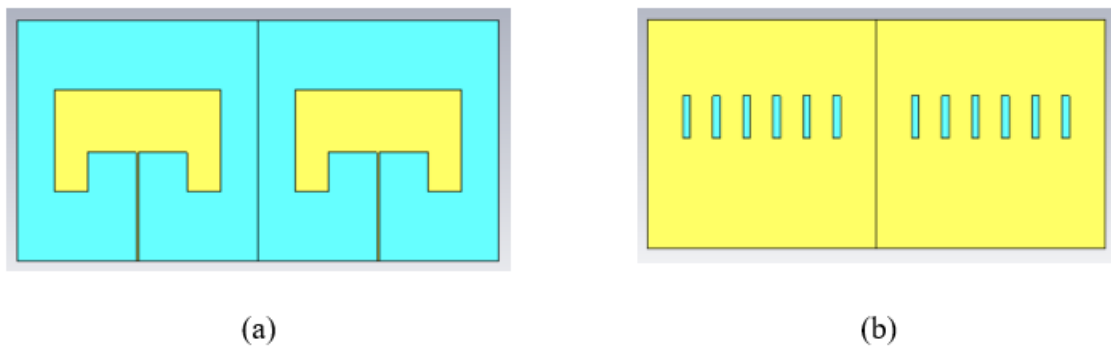


Figure 4.15: (a)Front view (b) Back view of 1 x 2 array antenna

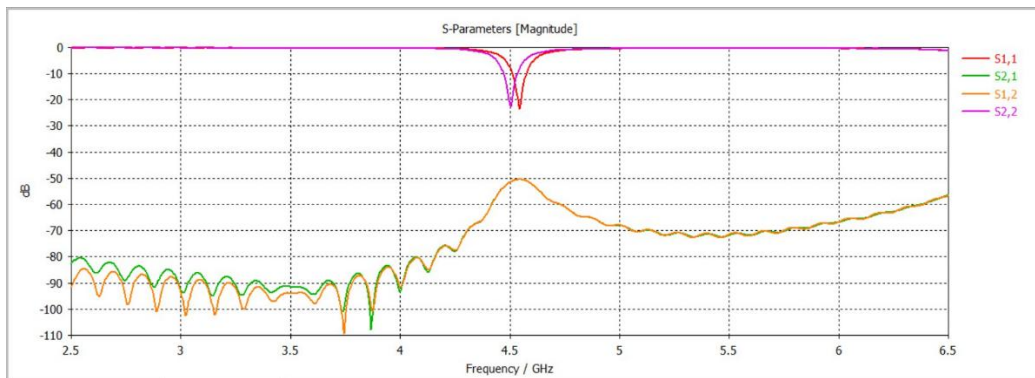


Figure 4.16: S-Parameter of 1 x 2 array antenna

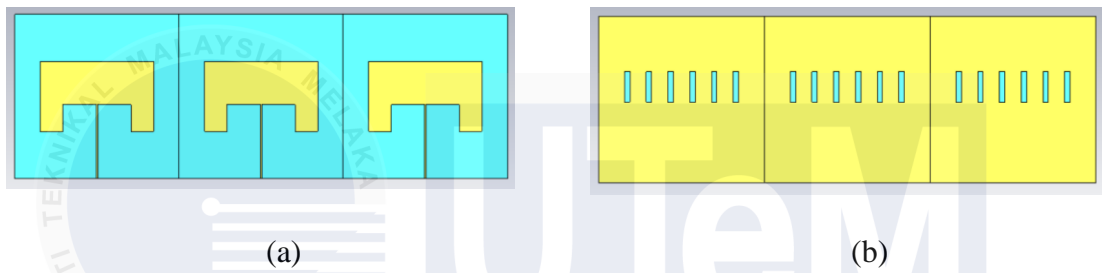


Figure 4.17: (a) Front view (b) Back view of 1 x 3 array antenna

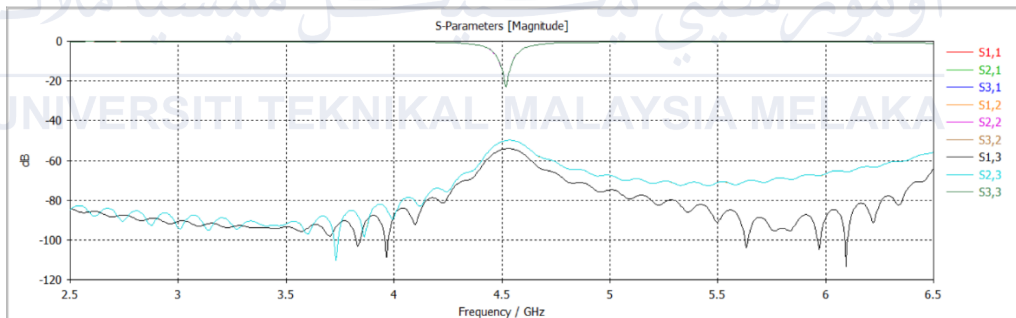


Figure 4.18: S-Parameter of 1 x 3 array antenna

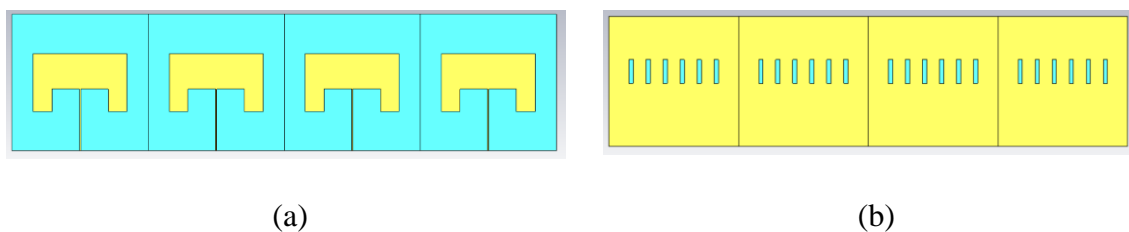


Figure 4.19: (a)Front view (b) Back view of 1 x 4 array antenna

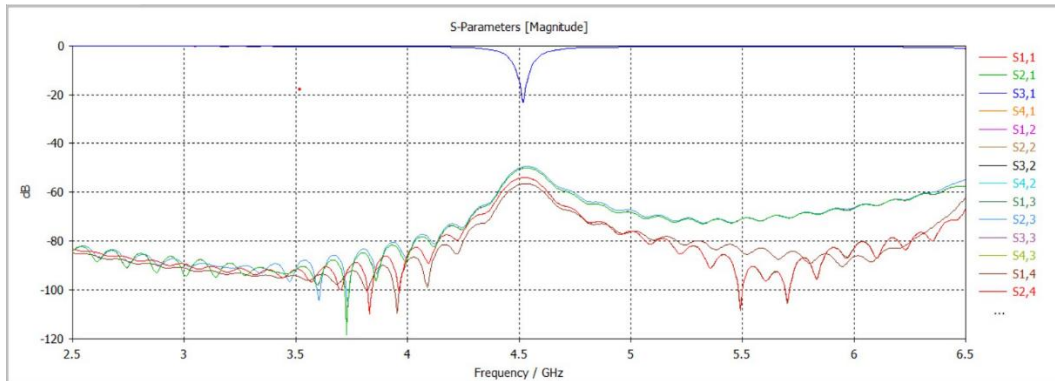


Figure 4.20: S-Parameter of 1 x 4 array antenna

4.6 Summary

MIMO (Multiple Input Multiple Output) antennas, particularly focusing on biomedical in a compact manner are thoroughly inscribed in this chapter. It emphasizes the difficulties that need to be addressed when including MIMO antennas in biomedical devices, including size, flexibility, and biocompatibility limitations. The research looks into a new way to use a PET substrate with a low dielectric constant to improve performance, longevity, biocompatibility, transparency, and flexibility to lessen the impact of these problems. In order to achieve conformability and efficient communication through the reduction of distance between sensors, it is necessary to use modern materials and creative fabrication techniques, as discussed in the article.

The results demonstrate a significant performance improvement when a Defected Ground Structure (DGS) is implemented. In the case of design with normal ground (Without DGS), the impedance matching, return loss, and total efficiency were less efficient. But for DGS, the operating frequency moved with the desired value (4.5 GHz) with a -19.84 dB return loss, lower VSWR which is 1.23, more surface current density (836.138 A/m), considerably higher total efficiency and gain. This was further supported by the comparison

of the S-parameter, bandwidth, and radiation pattern analysis of the results indicating significant enhancement in frequency selectivity and energy transmission.

Finally, the design extended to integrate some MIMO configurations such as 1×2 , 1×3 , and 1×4 linear arrays. The resulting arrays were scalable to deliver consistent bandwidth and better return loss, which indicates superior impedance matching and directional properties. We conclude this chapter by showing that these sophisticated designs are promising for high-performance biomedical antennas, thus enabling suitable applications in the field of wearable and/or implantable devices.



CHAPTER 5

CONCLUSION AND RECOMMENDATIONS

5.1 Conclusion

The project undertaken fulfilled in contributing to the advancement of antenna design in biomedicine. These insights are expected to lead to more reliable, effective, and efficient medical devices and provide a foundation for future developments in antenna technology based on refinements for specific medical applications.

Therefore, through the design and optimization process, resonance frequency was the main target, and it was proved that antennas can be engineered to provide high accuracy and very predictable performance metrics. Through the identification of critical parameters, including size, shape, and material properties.

The main contribution of this work covers an exhaustive performance analysis of the designed antenna for biomedical applications. This study focused on key factors like impedance matching, radiation patterns, and efficiency, which provides a thorough assessment of the antenna's compatibility with medical devices. This data can be observed which validate for use and the design of the proposed antenna performs at its optimal, thus meeting the stringent requirements of biomedical applications.

Overall, this project has successfully shown that advanced antenna design for biomedical applications can be carried out using simulation-based tools such as CST Studio Suite. The project focused on important aspects like resonance frequency, impedance matching, radiation patterns and efficiency and successfully solved them through accurate parameter optimization. These results highlight the importance of using simulation tools to design high-performance antennas that satisfy the high standards required for medical

purposes, without requiring fabrication for testing. Such contribution not only serves the antenna design community but also marks its game-changing effect in clinical utilities to evolve new, high-efficiency and reliable medical systems across the globe for better healthcare.

5.2 Potential for Commercialization

MIMO antenna technology is highly flexible and portable and is meant for commercialization and broader application in the biomedical field. Additionally, flexibility, compatibility with living organisms, and excellent communication skills fit the modern requirements of healthcare systems, especially the growing interest in wearable and implantable technology. The incorporation of the PET substrate enabled the integration of the antenna to the medical equipment without much interference thus presenting numerous opportunities for improving patients' comfort, and efficiency in monitoring the patients as well as increasing the effectiveness of treatment.

The commercialization of this technology will bring about the change in numerous biological uses like remote monitoring of patients, treatment methods, and diagnostic equipment. MIMO antenna system provides high-speed data transfer and reliable wireless communication. Many healthcare practitioners are in a position to transfer vital signs, medical imaging, and any other important information within a blink of an eye. This allows them to make sound decisions and quickly respond to any issue. In addition, the antenna shows high biocompatibility and robustness, which makes it more suitable for use for extended durations. This reduces the number of replacements made and hence helps to reduce the overall cost of healthcare.

To help this new gauge technology move from the research and development phase to the marketplace, medical manufacturing companies, hospitals, and regulatory health

departments would be approached for partnership. The collaboration of leading companies in this industry will incorporate the MIMO antenna system with existing and new biomedical equipment, and thus help this technology gain faster and broader market penetration. This means that engaging in regular cooperation with the authorities will guarantee the safety of all the parties help establish the new legislation and obtain the necessary permits more quickly. This will help to make it easier to deliver these revolutionary solutions to patients around the globe.

5.3 Future Works

For future improvements, the performance and estimation results of the biomedical MIMO antenna can be enhanced as follows:

i) The Technical Performance and cost analysis of proposed flexible substrate material alternatives.

- Further investigation into alternative flexible substrate materials, such as LCP or polyimide, to improve the performance, durability, and biocompatibility of the antenna. An investigation of the synergistic impact of combining different substrates on the performance characteristics of the antenna will greatly advance research in this field.

ii) Integrated Advanced Sensing Capabilities.

- In addition, another future avenue of research for the flexible MIMO antennas may be related to the provision of the advanced sensing elements. Unlike many present-day technologies focused on the collection of data and coupled with other equipment, this antenna will be equipped with sensors for measuring vital signs, the state of physiology, and the environment, ultimately turning it into a module for constant

health monitoring and data transfer. Such technologies are useful in the sense that they enhance the level of customization of the medical treatment being offered, make it possible to offer healthcare services remotely, and keep diseases from progressing to the later stages, a feat that squarely places patient care and the quality of life high up on the agenda.

iii) Miniaturization Techniques and New Antenna Geometries.

- Other possibilities may be researched in order to find other ways of miniaturization and other new placement options for an antenna to design biological antennas which are the smallest and less noticeable. Therefore, to meet this demand as well as fulfill the need for a medical device to blend smoothly in the actual lives of individuals, it would be very advantageous to develop miniature antennas with high efficiency and versatility. The resolution is as follows in modern fabrication techniques such as Additive Manufacturing or Nanotechnology, the development of miniature and high-performance antenna systems can be positively influenced.

REFERENCES

- [1] L. Gerold, H. Lutfi, and T. Spittler, "User's Perceived Attitudes and Acceptance Towards Wearable Devices in Healthcare," *European Journal of Medical and Health Sciences*, vol. 6, no. 1, pp. 10–16, Jan. 2024, doi: 10.24018/ejmed.2024.6.1.1990.
- [2] C. M. Vidhya, Y. Maithani, and J. P. Singh, "Recent Advances and Challenges in Textile Electrodes for Wearable Biopotential Signal Monitoring: A Comprehensive Review," Jul. 01, 2023, *Multidisciplinary Digital Publishing Institute (MDPI)*. doi: 10.3390/bios13070679.
- [3] M. N. Abbasi *et al.*, "Design and optimization of a transparent and flexible MIMO antenna for compact IoT and 5G applications," *Sci Rep*, vol. 13, no. 1, Dec. 2023, doi: 10.1038/s41598-023-47458-1.
- [4] H. Qiu *et al.*, "Compact, Flexible, and Transparent Antennas Based on Embedded Metallic Mesh for Wearable Devices in 5G Wireless Network," *IEEE Trans Antennas Propag*, vol. 69, no. 4, pp. 1864–1873, Apr. 2021, doi: 10.1109/TAP.2020.3035911.
- [5] Q. L. Li, S. W. Cheung, D. Wu, and T. I. Yuk, "Optically transparent dual-band mimo antenna using micro-metal mesh conductive film for WLAN system," *IEEE Antennas Wirel Propag Lett*, vol. 16, pp. 920–923, 2017, doi: 10.1109/LAWP.2016.2614577.
- [6] N. H. Sulaiman, M. I. Abbasi, N. A. Samsuri, M. K. A. Rahim, and F. C. Seman, "A Low-Profile Compact Meander Line Telemetry Antenna with Low SAR for Medical Applications," *Wirel Commun Mob Comput*, vol. 2022, 2022, doi: 10.1155/2022/7761150.
- [7] U. Ali, S. Ullah, B. Kamal, L. Matekovits, and A. Altaf, "Design, Analysis and Applications of Wearable Antennas: A Review," 2023, *Institute of Electrical and Electronics Engineers Inc.* doi: 10.1109/ACCESS.2023.3243292.
- [8] H. Khan, S. A. Ali, M. Wajid, and M. S. Alam, "Antenna array design on flexible substrate for wireless power transfer," *Frontiers in Engineering and Built Environment*, vol. 1, no. 1, pp. 55–67, Jul. 2021, doi: 10.1108/febe-03-2021-0018.
- [9] A. R. Chishti *et al.*, "Optically Transparent Antennas: A Review of the State-of-the-Art, Innovative Solutions and Future Trends," Jan. 01, 2023, *MDPI*. doi: 10.3390/app13010210.
- [10] C. Fernández-Prades, H. Rogier, A. Collado, and M. M. Tentzeris, "Flexible substrate antennas," 2012. doi: 10.1155/2012/746360.
- [11] M. A. S. M. Al-Haddad, N. Jamel, and A. N. Nordin, "Flexible Antenna: A Review of Design, Materials, Fabrication, and Applications," in *Journal of Physics: Conference Series*, IOP Publishing Ltd, Jun. 2021. doi: 10.1088/1742-6596/1878/1/012068.
- [12] J. Sashmitha and C. Poongodi, "PET-BASED FLEXIBLE ANTENNA WITH INKJET PRINTING FOR 5G WIRELESS APPLICATIONS," *International Research Journal of Modernization in Engineering Technology and Science*, Mar. 2023, doi: 10.56726/irjmets34430.
- [13] M. S. Islam, M. I. Ibrahimy, S. M. A. Motakabber, A. K. M. Z. Hossain, and S. M. K. Azam, "Microstrip patch antenna with defected ground structure for biomedical

application,” *Bulletin of Electrical Engineering and Informatics*, vol. 8, no. 2, pp. 586–595, Jun. 2019, doi: 10.11591/eei.v8i2.1495.

